Ruthenium(ii) arene complexes bearing simple dioxime ligands: effective catalysts for the one-pot transfer hydrogenation/N-methylation of nitroarenes with methanol

Published Version:
Colaiezzi, R., Saviozzi, C., di Nicola, N., Zacchini, S., Pampaloni, G., Crucianelli, M., et al. (2023). Ruthenium(ii) arene complexes bearing simple dioxime ligands: effective catalysts for the one-pot transfer hydrogenation/N-methylation of nitroarenes with methanol. CATALYSIS SCIENCE & TECHNOLOGY, 13, 2160-2183 [10.1039/d3cy00218g].

Availability:
This version is available at: https://hdl.handle.net/11585/925487 since: 2023-05-15

Published:
DOI: http://doi.org/10.1039/d3cy00218g

R. Colaiezzi, C. Saviozzi, N. Di Nicola, S. Zacchini, G. Pampaloni, M. Crucianelli, F. Marchetti, A. Di Giuseppe, L. Biancalana, "Ruthenium(II) Arene Complexes Bearing Simple Dioxime Ligands: Effective Catalysts for the One-Pot Transfer Hydrogenation/N-Methylation of Nitroarenes with Methanol", *Catal. Sci. Technol.*, **2023**, *13*, 2160-2183

Ruthenium(II) Arene Complexes Bearing Simple Dioxime Ligands: Effective Catalysts for the One-Pot Transfer Hydrogenation/*N*-Methylation of Nitroarenes with Methanol

Roberta Colaiezzi,[a,#] Chiara Saviozzi,[b,c,#] Nicola di Nicola,[a] Stefano Zacchini,[d] Guido Pampaloni,[b,c] Marcello Crucianelli,[a] Fabio Marchetti,[b,c] Andrea Di Giuseppe,[a]Lorenzo Biancalana,[b,c*]*

[a] *Università dell'Aquila, Dipartimento di Scienze Fisiche e Chimiche, Via Vetoio, I-67100 L'Aquila, Italy.*

[b] *Università di Pisa, Dipartimento di Chimica e Chimica Industriale, Via G. Moruzzi 13, I-56124 Pisa, Italy.*

[c] *Consorzio Interuniversitario Reattività Chimica e Catalisi (CIRCC), Via Celso Ulpiani 27, I-70126 Bari, Italy.*

[d] *Università di Bologna, Dipartimento di Chimica Industriale "Toso Montanari", Viale del Risorgimento 4, I-40136 Bologna, Italy.*

[#]these authors have contributed equally to the work.

Corresponding Author(s)

* E-mail: lorenzo.biancalana@unipi.it, andrea.digiuseppe@univaq.it

Abstract.

The reductive *N*-monomethylation of nitroarenes is a reactionof wide scientific interest that can be conveniently realized in one-pot using methanol as both the reductant (H_2 donor), alkylating agent (CH_3^+ donor) and solvent. Ruthenium(II) η^6-arene complexes are increasingly investigated as efficient catalytic precursors for (transfer) hydrogenation and dehydrogenation processes. In this framework, amino or alcohol groups working as proton-relay units are essentialto realizea metal-ligand cooperative catalysis. Herein, starting from commercially available and inexpensive dioxime ligands, $\{RC{=}N(OH)\}_2$, we developed novel ruthenium(II) arene complexes that efficiently catalyze the tandem reduction/*N*-methylation of aromatic nitrocompounds with methanol.

Thus, the complexes $[RuX(\kappa^2N\text{-dioxime})(\eta^6\text{-}p\text{-cymene})]^+$ (Cl/dimethylglyoxime, $[\mathbf{1}]^+$; Cl/nioxime, $[\mathbf{2}]^+$; I/nioxime, $[\mathbf{3}]^+$), $[RuCl(\kappa^2N\text{-dioxime})(\eta^6\text{-}C_6Me_6)]^+$ (dimethylglyoxime, $[\mathbf{4}]^+$; nioxime, $[\mathbf{5}]^+$; diphenylglyoxime, $[\mathbf{6}]^+$) and $[RuCl(\kappa^2N\text{-nioxime})(\eta^6\text{-}1,3,5\text{-}C_6H_3Me_3)]^+$ ($[\mathbf{7}]^+$) were isolated as nitrate or hexafluorophosphate salts in high yields and characterized by analytical (CHN content, conductivity) and spectroscopic (IR, NMR) techniques.Furthermore, three zwitterionic oxime-oximato derivatives were prepared ($\mathbf{2^{-H}}$-$\mathbf{4^{-H}}$) and the crystal structures of both dioxime ($[\mathbf{3}]^+$, $[\mathbf{4}]^+$) and oxime-oximato ($\mathbf{4^{-H}}$) complexes were elucidated by X-ray diffraction.

Following optimization of the reaction conditions for the one-pot reduction/*N*-methylation of nitrobenzene as benchmark substrate (MeOH, ^{t}BuOK, 130 °C, 18 h), the catalytic activity of the dioxime complexes $[\mathbf{1}$-$\mathbf{7}]^+$and selected ruthenium(II) compounds for comparative purposeswas assessed. The best catalytic precursor, $[\mathbf{3}]NO_3$, was effective in the conversion of a series of aromatic nitrocompounds into the respective *N*-methyl anilines, which were isolated as hydrochloride salts following silica chromatography. NMR and MS experiments carried out on the model catalytic system (nitrobenzene/$[\mathbf{3}]NO_3$) confirmed the role of methanol as C_1 and H_2 source andgave insights about organic intermediates. Following *in situ* bis-deprotonation to the dioximato complex $[\mathbf{3^{-2H}}]^-$, displacement of the η^6-arene ligand is proposed as the activation step of the pre-catalyst.

Keywords. homogeneous catalysis; ruthenium arene complexes; dioxime; borrowing hydrogen; amine methylation; nitroarene reduction; transfer hydrogenation; *N*-methyl aniline; metal-ligand cooperativity

1. Introduction.

N-methyl anilines find application as building blocks or additives for dyes, polymers, explosives, herbicides and fuels.[1] They are usually obtained by methylation of the parent aniline. In a broader context, methylation of NH groups represents an important late-stage functionalization for a variety of fine chemicals and pharmaceuticals.[2] In order to avoid the use of critically hazardous methylating agents (*e.g.* MeI, Me_2SO_4, methyl triflate), a convenient,atom economicalmethod for the synthesis of *N*-methyl anilines (amines) is represented by the use of *methanol* in a *borrowing hydrogen* approach (Scheme 1).[3] In this reaction, methanol is formally involved in a dehydrogenation/condensation/hydrogenation sequence, releasing water as the sole co-product. However, the dehydrogenation of methanol (ΔH° = +130.5 kJ/mol) is more challenging with respect to other commonly employed alkanols such as ethanol (ΔH° = +85.9 kJ/mol), isopropanol (ΔH° = +70.0 kJ/mol) or benzylic alcohol (ΔH° = +73.7 kJ/mol).[4]

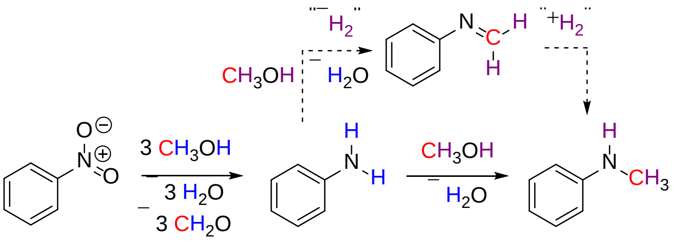

Scheme 1. Nitrobenzene hydrogenation and aniline *N*-methylation using methanol as C_1 and H_2 source. Imine intermediate is indicated by the dotted arrows.

Ruthenium complexes are renowned for catalyzing such H_2-autotransfer processes, including *N*-alkylation of amines with alcohols.[5] Thus, from the pioneering work of Watanabe and co-workers

(1988,employing RuCl$_3$/P(O^{t}Bu)$_3$),[6] several Ru-based systems for the catalytic*N*-methylation of alkyl or arylamines with methanol have been reported,[7] with a recent focus on ruthenium(II) η^6-arene precursors.[8] From a catalyst design perspective, the introduction of ancillary (non-coordinating) OH or NHMe groups on polydentate *N*-donor ligandsresulted in an improved catalytic performancein some cases (**Ru1-Ru3** in Scheme 2).[7e-f,8d] Cooperative effects from peripheral hydroxyl groups were also observed for a pentamethylcyclopentadienyl (Cp*) iridium(III) catalystinvestigated for the same process (**Ir1** in Scheme 2).[9]

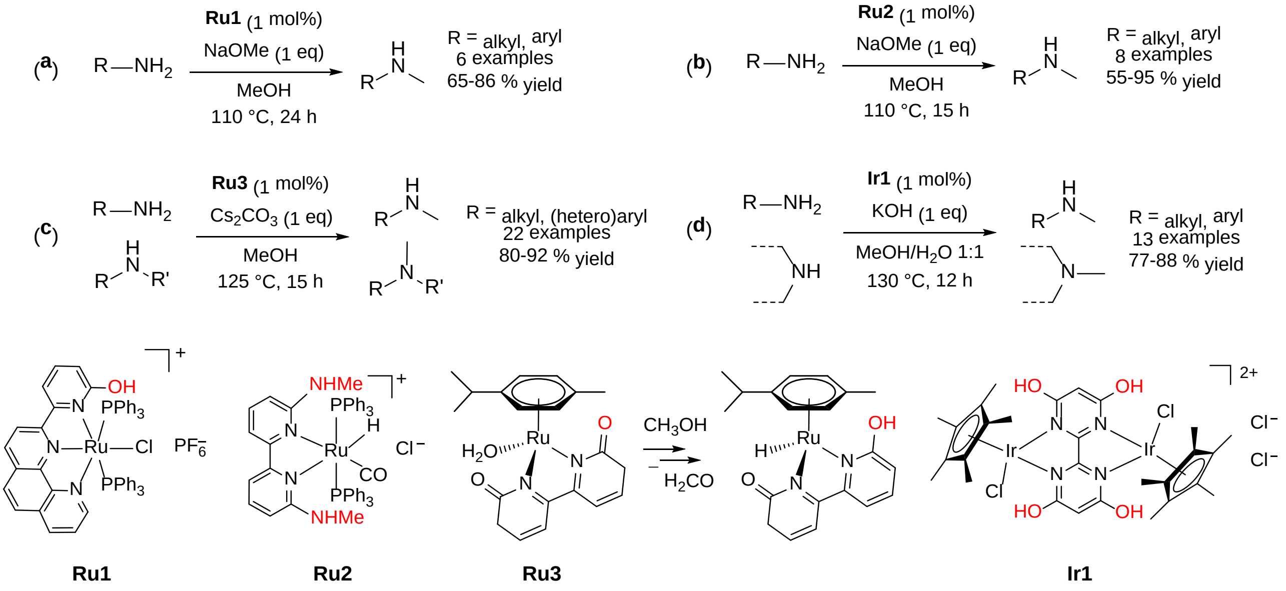

Scheme 2. Literature catalytic systems for the *N*-methylation of amines (anilines), taking advantage of cooperative effects from ancillary hydroxy or amino functions (in red) on the catalyst precursors **Ru1** (**a**, 2018), **Ru2** (**b**, 2018), **Ru3** (**c**, 2021) or **Ir1** (**d**, 2020). Year of publication in blue.

The hydrogenationof easily-available nitroarenes is probably the most common method to access the respective aniline, including some industrially-relevant cases.[10] Therefore, an efficient one-pot process for the preparation of *N*-methyl anilines from the respective nitroarenes with methanol acting simultaneously as the solvent, C_1 synthon and H_2 donorwould be highly attractive (Scheme 1). Ruthenium complexes achieved great success as homogeneous catalytic precursors for the transfer hydrogenation of variety of organic substrates.[11] Nevertheless, to the best of our knowledge, only four Ru-based catalytic systems have been assessed for the one-pot reductive *N*-

methylation of nitroarenes (Scheme3).[12] These protocols operate under solvothermal conditions (110-130 °C) for 12-48 h and require a (super)stoichiometric amount of a strong Brønsted base that – in principle – should function as a co-catalyst. Such base loading and temperature requirements are frequently encountered also in thecatalytic *N*-methylation of amines/anilineswith methanol (see Scheme 2 for instance).[5b] The catalytic precursors **Ru4-Ru6** feature elaborated κ^3 *N* pincer-type ligands. Alternatively, commercial $RuCl_3 \cdot nH_2O$ was employed at a very high loading. Interestingly, a remote hydroxyl group of the bis-pyrazolyl-pyridine ligand in **Ru6** drastically improved the catalytic efficiency, being involved in key hydrogen bonding interactions during all steps of the DFT-optimized catalytic cycle.[12d]

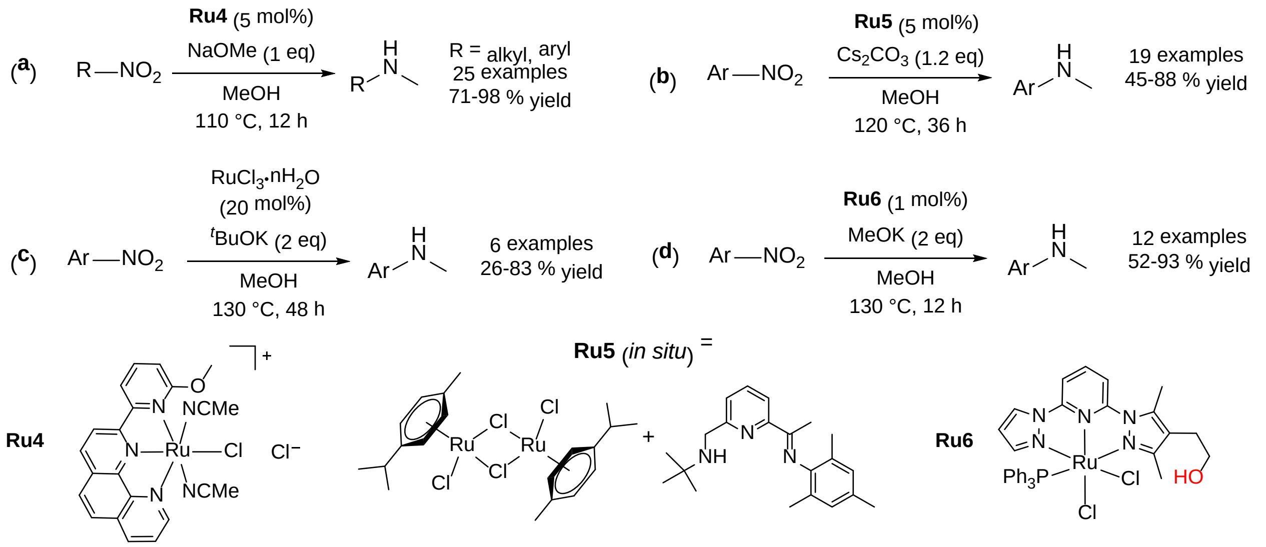

Scheme3. Catalytic systems for the tandem reductive *N*-methylation of nitro compounds employing Ru-based catalytic precursors **Ru4** (**a**, 2017), **Ru5** (**b**, 2019), $RuCl_3$ hydrate (**c**, 2021) or **Ru6** functionalized with a peripheral hydroxyl group (**d**, 2022). Year of publication in blue.

As part of our ongoing interest in the development of ruthenium(II) η^6-arene complexes employing simple, commercially-available ligands within the framework of metal-ligand bifunctional catalysis,[13] we turned our attention to *dioxime* ligands, which combine a chelating *N,N* unit with ancillary (and potentially non-coordinating) OH groups (Figure 1).

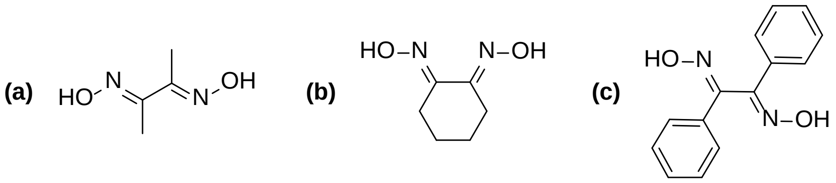

Figure 1. Commercially available dioxime ligands employed in this work: dimethylglyoxime (dimethyldioxime) **(a)**, nioxime (1,2-cyclohexanone dioxime) **(b)**, diphenyldioxime **(c)**.

Transition metal complexes of dioximes display a rich coordination chemistry[14] and those of cobalt(III) have been extensively investigated as models of cobalaminor electrocatalysts for H_2 production.[15] The use of dimethylglyoxime and nioxime (1,2-cyclohexanone dioxime) as gravimetric reagents for the analysis ofnickel dates back to 118 and 75 years ago, respectively.[16] Nevertheless, investigations on the catalytic activity of dioxime complexes of ruthenium have been practically ignored up to this date.[17] In this respect, ruthenium(II) arene complexes featuring bidentate amino-, pyridyl- and phosphane-(mono)oxime ligands have been tested for the transfer hydrogenation of ketones and nitroarenes, dehydrogenation of hydrazine and alkyne hydration (Figure 2a).[18] Curiously, the NOH/NO^- moiety was relegated to a passive role in the proposed mechanisms, even when the oxime complexes outperformed structurally-similar compounds in terms of catalytic activity.[18c,d] Furthermore, relatively few dioxime complexes of other 4d and 5d metals have been investigated for their catalytic activity.[19] Among them, a notable case is represented by *in situ* formed Ir(III) Cp* complexes with amino-substituted dioxime ligands, whichwere recently reported to be highly efficient for the dehydrogenation of aqueous formic acid (Figure 2b).[20]

Herein we employed commercially available dioximes for the preparation of an unprecedented series of mononuclear ruthenium(II) compounds comprising different arene and halide co-ligands and counter ions (Figure 2c). The catalytic activity of the complexes in the tandem reduction /*N*-methylation of nitroarenes with methanol was investigated, revealing a key role of the dioxime ligand for the selectivity of the process.

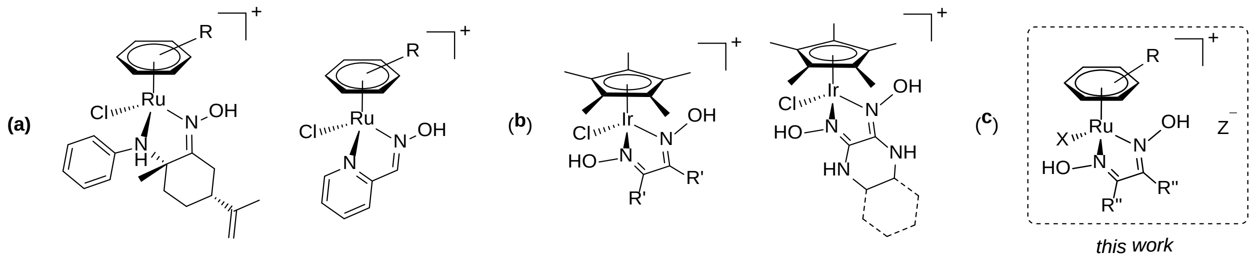

Figure 2. Previously-reported Ru(II) arene complexes (arene = C_6H_6, *p*-cymene) with pyridyl-oxime or amino-oxime ligands(**a**)and Ir(III) Cp* dioxime complexes (R' = H, Me, Cl, NH_2, NH^iPr) (**b**) investigated as catalytic precursors (Cl^- salts). General structure of the ruthenium(II) dioxime compounds investigated in this work (arene = *p*-cymene, C_6Me_6, 1,3,5-$C_6H_3Me_3$; X = Cl, I; Z = NO_3, PF_6; R'' as in Figure 1) (**c**).

2. Results and discussion.

2.1.Synthesis and characterization of Ru compounds.

Ruthenium arene dioxime complexes $[RuX(dioxime)(\eta^6\text{-arene})]^+$, $[\mathbf{1\text{-}7}]^+$, were prepared by a two-step procedure involving cleavage of the halido-bridged dimers $[RuX_2(\eta^6\text{-arene})]_2$ (arene/X: *p*-cymene/Cl, **D1**; *p*-cymene/I, **D2**; C_6Me_6/Cl, **D3**; 1,3,5-$C_6H_3Me_3$/Cl, **D4**) with $AgNO_3$ in MeCN or MeOH followed by addition of the selected dioxime at room temperature (at reflux for $[RuCl_2(\eta^6\text{-}1,3,5\text{-}C_6H_3Me_3)]_2$; Scheme 4). The reactions were performed under rigorous stoichiometric conditions: excess $AgNO_3$ led to the formation of by-products (*vide infra*) while excess dioxime could not be easily removed during work-up. Notably,the interaction of the putative $[RuX(MeCN)_2(\eta^6\text{-}p\text{-cymene})]^+$ (X = Cl, I) intermediates[21] with nioximealways resulted in a variable (5-20%) release of *p*-cymene and consequent formation of unidentified nioxime complexes. The successful preparation of [**2-3**]NO_3 required MeOH as solvent for both reaction steps. Compounds [**1-7**]NO_3 were isolated as air-stable yellow/orange powders in 77−93 % yields. Similarly, theone-pot reaction of $[RuCl_2(\eta^6\text{-arene})]_2$ (arene = *p*-cymene, C_6Me_6) with KPF_6 and nioxime in EtOH led to the isolation of $[\mathbf{2}]^+$ and $[\mathbf{6}]^+$ as PF_6^-salts in 82−85 % yields (Scheme 4). These two compounds were prepared as an alternative to the nitrate salts.

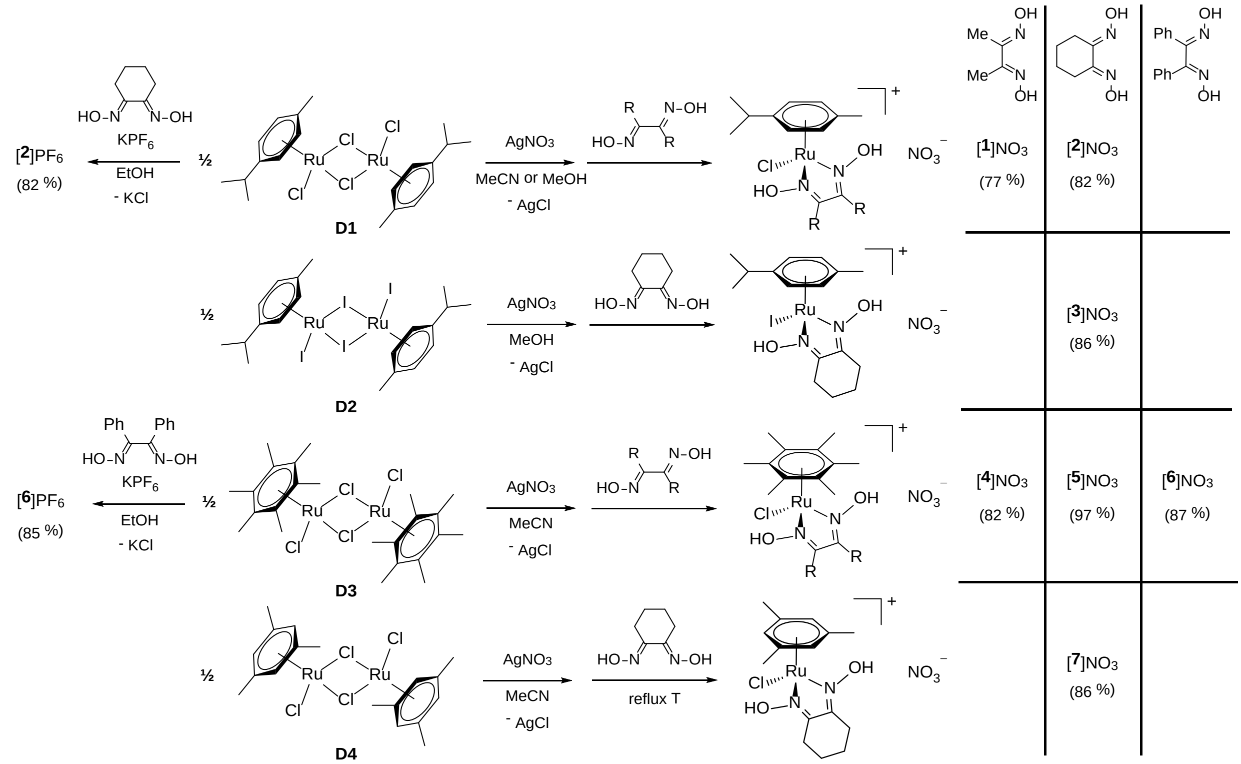

Scheme 4. Preparation of ruthenium η^6-arene dioxime complexes [**1-7**]$^+$ from the corresponding halido-bridged dimers **D1-D4**. All reactions were carried outin stoichiometric conditions at room temperature, except where otherwise noted. Isolated yields (as NO_3^- or PF_6^- salts) in parentheses.

To the best of our knowledge, [**1**-**7**]$^+$ represent the first examples of ruthenium arene complexes with dioxime-type ligands. Compounds [**1**-**7**]NO_3 and [**2**,**6**]PF_6 were characterized by analytical (CNH content, molar conductivity) and spectroscopic (IR, NMR, UV-Vis) techniques; IR and NMR spectra are displayed in Figures S5-S28 in the Supporting Information. The ^{1}H and ^{13}C NMR spectra of [**1**-**7**]$^+$ in CD_3OD are in keeping with the C_s symmetry of the cations.[22] The ^{13}C NMR resonance of the CN group of the dioxime ligand underwent a considerable deshielding upon coordination, being detected in the 160-165 ppm range for [**1**-**7**]$^+$ and around 155 ppm for the free dioximes (Table S1). The same effect was noticed for the NCH_x groups of dimethylglyoxime and nioxime, indicatinga predominant σ-donation over π-back donation in the bonding with the metal center.[23] Solid-state IR spectra of [**1**-**7**]NO_3 and [**2**,**6**]PF_6 show broad absorptions in the 3000-3400 cm^{-1} region related to O-H stretching and a diagnostic sharp band at 1030-1090 cm^{-1} due to the N-O vibration.[24,25] Conversely, C=N stretching bandswere not found in the expected 1500-1600 cm^{-1} region[18e,26] for both the dioxime ligands and their Ru complexes. The NO_3^- ion manifested itself with a strong IR absorption peaking at 1250-1270 cm^{-1}and a ^{14}N NMR resonance around – 4 ppm. Similarly, thePF_6^- ion gave rise to anintense IR band at 830 cm^{-1} and the typical patterns in the ^{19}F and ^{31}P NMR spectra.

The molecular structures of the cations [**3**]$^+$ and [**4**]$^+$ were determined by single crystal X-ray diffraction (SC-XRD) on their [**3**]NO_3 and[**4**]$NO_3{\cdot}H_2O$ salts. More precisely, crystals of the latter were grown from an EtOH solution of [**4**]NO_3 spiked with HNO_3. Indeed, a previous crystallization attempt of [**4**]NO_3 in EtOH gave the structure of its deprotonated, neutral derivative **4^{-H}**, corresponding to a formal loss of HNO_3. The structures of [**3**]$^+$, [**4**]$^+$ and **4^{-H}** are reported in Figures 3-5, whereas the main bonding parameters are summarized in Table 1. These complexes adopt the expected three-legged piano-stool geometry, with one coordination site occupied by the halide and the other two sites by the bidentate dioxime ([**3**]$^+$ and [**4**]$^+$) oroxime-oximato (**4^{-H}**) ligand. All the bonding parameters of [**3**]$^+$ and [**4**]$^+$ are perfectly comparable and the dioxime ligands bind the Ru centers in a symmetric way. The presence of H-atoms on both oxygens of dioxime ligands of [**3**]$^+$ and [**4**]$^+$ is corroborated by the extended H-bond network found in their structures (Figures S29-S30, Tables S2-S3). The crystal structure of **4^{-H}**$\cdot 1.5H_2O$ contains two independent **4^{-H}** molecules displaying almost identical geometries and bonding parameters. The neutral charge of the complex is supported by the absence of any counter-ion. In addition, an extended H-bond network involves the protonated OH and deprotonated O groups of the oxime-oximato ligand as well as the co-crystallized H_2O molecules and the chloride ligand (Figure S31, Table S4). Deprotonation of O(2) causes an asymmetry within the bonding parameters of theoxime-oximato ligand. Indeed, the N(2)-O(2) contact of **4^{-H}** [1.305(2) and 1.304(2) Å for the two independent molecules] is considerably shorter than N(1)-O(1) [1.401(2) and 1.394(2) Å]. For comparison, the cationic complexes [**3**]$^+$ and [**4**]$^+$ display intermediate values for both N(2)-O(2) [1.378(3) and 1.379(4) Å for [**3**]$^+$ and [**4**]$^+$, respectively] and N(1)-O(1) [1.378(3) and 1.371(4) Å] contacts. It must be remarked that the C(1)-N(1) [1.298(4), 1.288(5), 1.296(2) and 1.296(3) Å for [**3**]$^+$, [**4**]$^+$ and the two independent molecules of **4^{-H}**]and C(1)-C(2) [1.453(5), 1.458(5), 1.446(3) and 1.448(3) Å] distances are almost unchanged in the three complexes. In contrast, a slight elongation is observed for the C(2)-N(2) bonding contact of **4**$^{\mathbf{-H}}$ [1.314(2) and 1.318(3) Å for the two independent molecules] compared to [**3**]$^{+}$ [1.298(4) Å] and [**4**]$^{+}$ [1.290(5) Å]. Moreover, the Ru(1)-N(1) [2.0479(16) and 2.0484(16) Å for the two independent molecules] and Ru(1)-N(2) [2.0438(16) and 2.0550(16) Å] bonds of **4**$^{\mathbf{-H}}$ do not display an appreciable asymmetry and, indeed, they are also comparable to the values found in the cations [**3**]$^{+}$ [2.051(3) and 2.058(3) Å for Ru(1)-N(1) and Ru(1)-N(2), respectively] and [**4**]$^{+}$ [2.057(3) and 2.061(3) Å].All bonding parameters are comparable to those found in related Ru complexes containing dioxime andoxime-oximato ligands.[25,27]

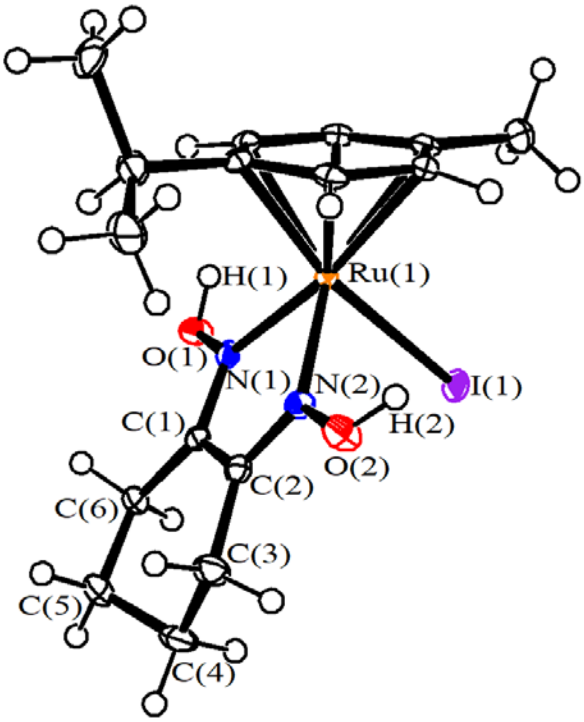

Figure 3. Molecular structure of [**3**]$^{+}$ in [**3**]NO_3. Displacement ellipsoids are at the 50% probability level.

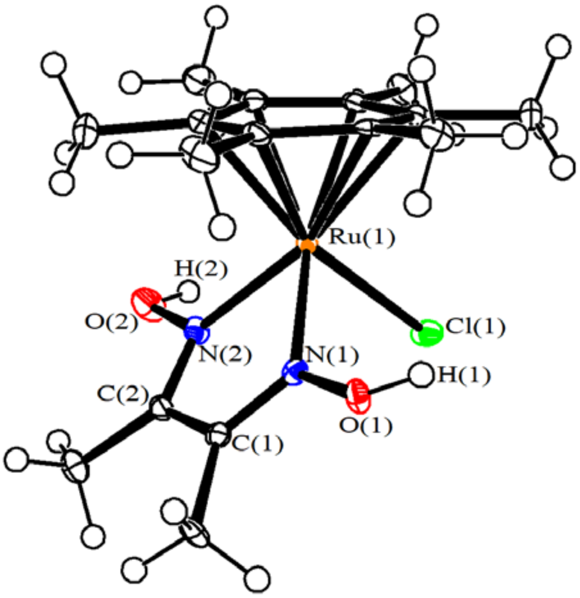

Figure 4. Molecular structure of [**4**]$^+$ in [**4**]$NO_3 \cdot H_2O$. Displacement ellipsoids are at the 50% probability level.

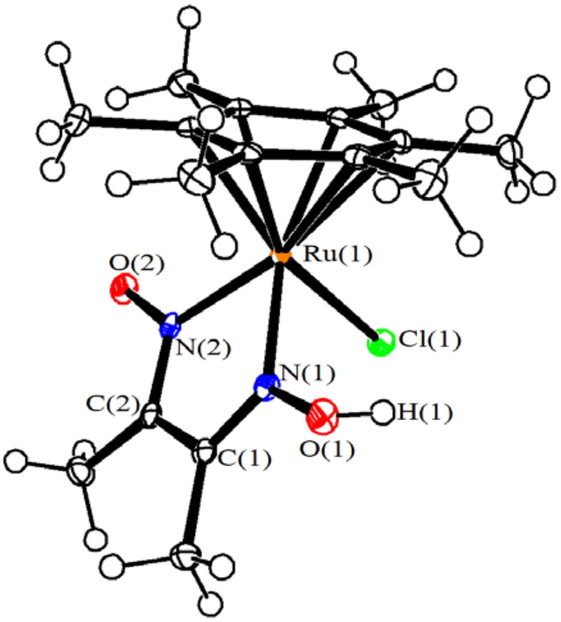

Figure 5. Molecular structure of **4**$^{-H}$ in**4**$^{-H}$**·**1.5H_2O. Displacement ellipsoids are at the 50% probability level.

Table 1. Selected bond lengths (Å) and angles (°) for [**3**]NO_3, [**4**]NO_3 and **4**$^{-H}$.

	[**3**]NO_3	[**4**]NO_3	**4**$^{-H}$	**4**$^{-H}$
			Molecule 1	Molecule 2
Ru(1)-X(1)	2.6986(10)	2.4107(11)	2.4093(5)	2.4259(5)
Ru(1)-N(1)	2.051(3)	2.058(3)	2.0479(16)	2.0484(16)
Ru(1)-N(2)	2.057(3)	2.061(3)	2.0438(16)	2.0550(16)
Ru(1)-C_{arene}^{av}	2.217(7)	2.222(10)	2.226(5)	2.224(5)
N(1)-O(1)	1.378(3)	1.371(4)	1.401(2)	1.394(2)

N(2)-O(2)	1.378(3)	1.379(4)	1.305(2)	1.304(2)
C(1)-N(1)	1.298(4)	1.288(5)	1.296(2)	1.296(3)
C(2)-N(2)	1.298(4)	1.290(5)	1.314(2)	1.318(3)
C(1)-C(2)	1.453(5)	1.458(5)	1.446(3)	1.448(3)
N(1)-Ru(1)-N(2)	74.40(11)	73.66(12)	75.26(6)	75.69(6)
Ru(1)-N(1)-C(1)	119.8(2)	119.3(2)	118.66(13)	118.63(13)
Ru(1)-N(2)-C(2)	119.0(2)	119.9(3)	117.99(13)	122.75(12)
N(1)-C(1)-C(2)	112.9(3)	113.7(3)	113.80(17)	114.05(17)
N(2)-C(2)-C(1)	113.9(3)	112.4(3)	113.72(17)	114.25(17)
C(1)-N(1)-O(1)	113.3(3)	114.9(3)	115.88(15)	115.35(16)
C(2)-N(2)-O(2)	113.9(3)	115.5(3)	118.87(16)	119.88(16)
Ru(1)-N(1)-O(1)	126.7(2)	125.4(2)	125.45(11)	125.86(12)
Ru(1)-N(2)-O(2)	127.1(2)	124.0(2)	123.08(12)	122.75(12)

The results of the SC-XRD study highlighted the Brønsted acidity of the coordinated dioximes.[18a,26a,27a,28] Subsequently, oxime-oximato complexes **2**$^{-\mathbf{H}}$-**4**$^{-\mathbf{H}}$ were prepared in one-pot from the corresponding halido-bridged dimers **D1**-**D3** by sequential addition of the dioxime and $NaHCO_3$ or Ag_2O in MeOH at room temperature, in stoichiometric conditions (Scheme 5). For simplicity, the structuresof these zwitterionic complexes are drawn with a negative charge on the oxygen atom. Nevertheless, in accordance with SC-XRD data on **4**$^{-\mathbf{H}}$, some electron delocalization in the O-N-C fragment should be considered to best describe the structure of the ligand.

Compounds **2**$^{-\mathbf{H}}$-**4**$^{-\mathbf{H}}$ were isolated as yellow/orange powders in 78-91 % yields and characterized as previously described; IR and NMR spectra are displayed in Figures S32-S40.Conductivity measurements in MeOH are in good agreement with the non-ionic nature of thecomplexes.A single set of signals was observed in the ^{1}H and ^{13}C NMR spectra of **2**$^{-\mathbf{H}}$-**4**$^{-\mathbf{H}}$ in CD_3OD, showing isochronous signals within the *p*-cymene and dioximefragments due torapid H^+/D^+ exchange in the NMR timescale. On comparison with [**2-4**]$^+$, the^{1}H NMR resonances of **2**$^{-\mathbf{H}}$-**4**$^{-\mathbf{H}}$ exhibit a characteristic shielding (*protonation shift*[29]) while the ^{13}C NMR resonance of the CN group becomes downfield shifted (Figure S41, Table S1). The solid-state IR spectra oftheoxime-oximato complexes show two strong bands around 1030-1040 and 1100-1110 cm^{-1}which can be assigned to the stretching vibrations of the different NO bonds,[26a,27c] in keeping with the X-ray structural analysis of **4**$^{-\mathbf{H}}$.

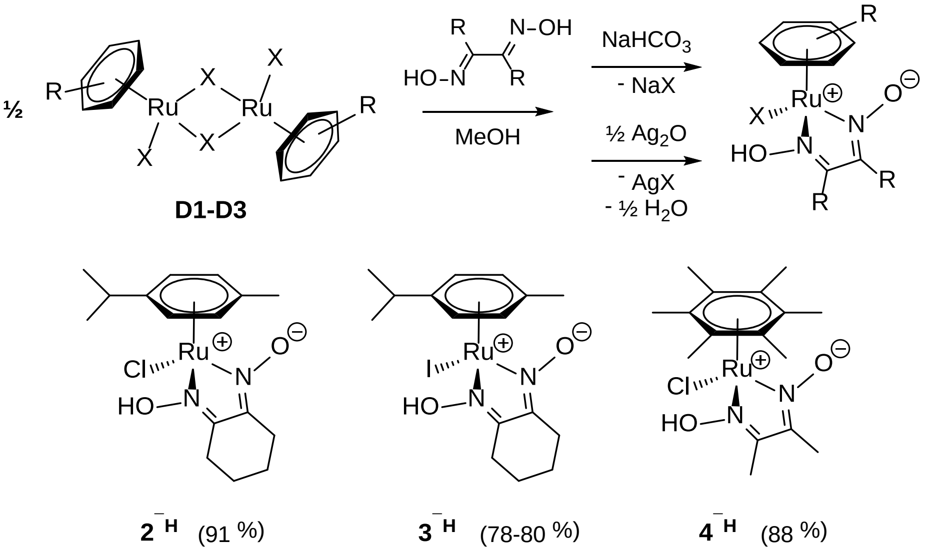

Scheme 5. One-pot synthesis of oxime-oximato complexes **2**$^{-H}$-**4**$^{-H}$ from the respective halido-bridged dimers **D1-D3**. Reactions were carried out at room temperature in stoichiometric conditions. Isolated yields in parentheses.

2.2. Reactivity of dioxime complexes in methanol.

In principle, $[RuX(\kappa^2 N\text{-}\{RC{=}NOH\}_2)(\eta^6\text{-arene})]^+$ (X = Cl, I) complexes possess two Brønsted-acidic groups (OH) and a halido ligand that could be replaced by a solvent molecule or the *N*-oxy group of another complex, giving rise to bimetallic oximato-bridged species.[30] Thenetwork of acid/base and halide/solvent equilibria (and associated compound naming)is represented in Scheme S1.These equilibria appearto be rather suppressed in methanol. Indeed,the largely predominant species in solution is the undissociated cationic dioxime complex [**1-7**]$^+$, as indicated by the presence of a unique set of signals in the ^{1}H NMR spectra of [**1-7**]NO_3 and [**2**,**6**]PF_6, the absence of the diagnostic signal for the chloride ion in the^{35}Cl NMR spectra of [**1**,**5**,**6**]NO_3 and [**2**]PF_6, and conductivity data of [**2**,**4**]NO_3 being in agreement with that of a reference 1:1 electrolyte (KNO_3).[31] The identity of [**3**]$^+$ in MeOH was further corroborated by ESI-MS (Figure S42). Subsequently, reactions of representative dioxime complexes ([**2**]PF_6 and [**3-4**]NO_3) in methanol with various Brønsted bases (Et_3N, $NaHCO_3$, K_2CO_3 or ^{t}BuOK) were investigated by ^{1}H NMR (see Experimental and ESI for details). Complexes [**2-4**]$^+$ can be deprotonated once or twice (Scheme 6a), judging by the progressive shielding of the ^{1}H NMR resonances (Figures S43-S45). Formation of the dioximato complex $[\mathbf{3}\text{-}^{\mathbf{2H}}]^{-}$ from $[\mathbf{3}]^{+}$ and ^{t}BuOK (3.0 eq.) was also checked by ESI-MS (as $K_2[\mathbf{3}^{\mathbf{-2H}}]^{+}$, Figure S46).

The species derived from chlorido/iodido dissociation from the two *p*-cymene complexes were not observed in solution, as confirmed by their independent preparation from $[Ru(NO_3)_2(\eta^6\text{-}p\text{-cymene})]$, nioxime and ^{t}BuOK (Scheme 6b, Figure S47). Interestingly, the major species formed upon double deprotonation of "$[Ru(MeOH)(nioxime)(p\text{-cymene})]^{2+}$" ($[\mathbf{3}_{\boldsymbol{MeOH}}]^{2+}$) lacks the C_s-symmetry, as indicated by its ^{1}H NMR set of signals, suggesting a dimeric dioximato-bridged nature ($\mathbf{3}_{\boldsymbol{dimer}}$). In this respect, the reactivity of $[\mathbf{2}\text{-}\mathbf{3}]^{+}$ is reminiscent of that recently described for $[IrCl(\eta^5\text{-}C_5H_5)(\kappa^2 N\text{-}\{CH_3C{=}NOH\}_2)]Cl$.[30b] Conversely, the second deprotonation of the hexamethylbenzene complex $[\mathbf{4}]^{+}$ is associated with the appearance of a second set of ^{1}H NMR signals, possibly related to chloride release from the dioximato species $[\mathbf{4}^{\mathbf{-2H}}]^{-}$.

Methanol (CD_3OD) solutions containing either $[\mathbf{3}]^{+}$, $\mathbf{3}^{\mathbf{-H}}$ and $[\mathbf{3}^{\mathbf{-2H}}]^{-}$ are relatively inert at room temperature for several hours. Instead, those obtained from $[Ru(NO_3)_2(\eta^6\text{-}p\text{-cymene})]$/nioxime/^{t}BuOK and corresponding to a formal halide removal from $[\mathbf{2},\mathbf{3}]^{+}$, $\mathbf{2},\mathbf{3}^{\mathbf{-H}}$ and $[\mathbf{2},\mathbf{3}^{\mathbf{-2H}}]^{-}$, are much less so. Indeed, traces of *p*-cymene were detected in the freshly prepared solutions and its relative amount increased over time (Figure S48). Besides, the solid isolated from the $[Ru(NO_3)_2(\eta^6\text{-}p\text{-cymene})]$/nioxime reaction (formally corresponding to $[\mathbf{3}_{\boldsymbol{MeOH}}][NO_3]_2$ in Scheme 6b) decomposed over a few days with complete release of *p*-cymene. Treatment of methanol solutions containing $[\mathbf{2}\text{-}\mathbf{3}]^{+}$, $\mathbf{3}^{\mathbf{-H}}$or $[\mathbf{3}^{\mathbf{-2H}}]^{-}$ with $AgNO_3$ immediately produced a significant amount of *p*-cymene (6-30 %; Figure S49) which became quantitative after some hours at room temperature. Overall, these results suggest thatthe dissociation or absence of the halido ligand results in the labilization of the *p*-cymeneligand in methanol.[32] Consistently with this hypothesis and with the greater lability of Ru−Cl bonds with respect to Ru−I,[33] reactions of the chloride analogue $[\mathbf{2}]^{+}$ with Brønsted bases often caused apartial cleavage of *p*-cymene.[34]

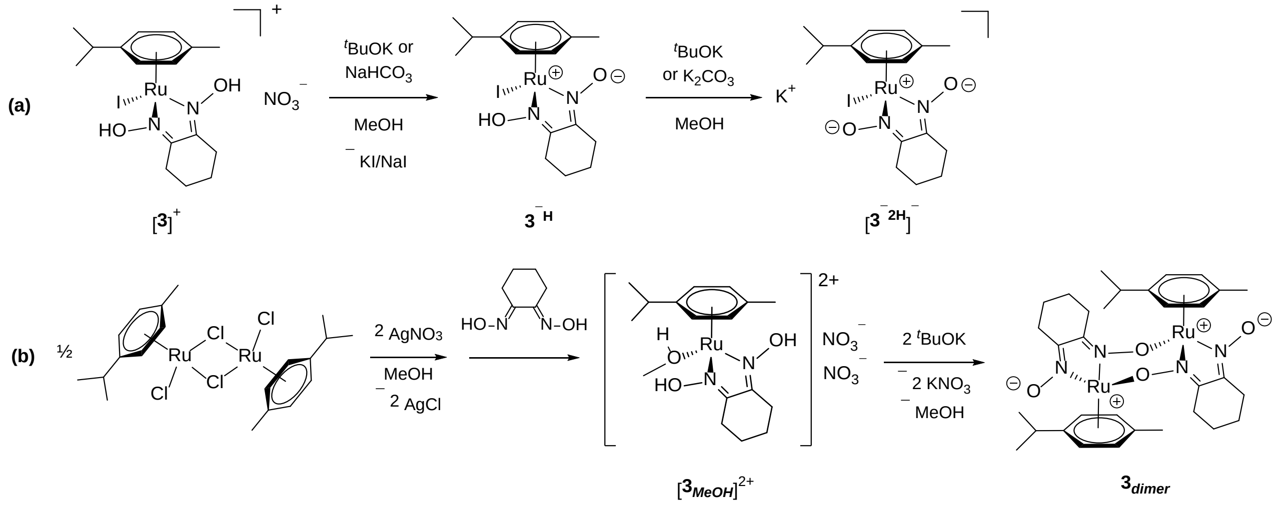

Scheme 6. Overview ofthe reactionsobserved in methanolic solutions of representative dioxime complexes.Sequential deprotonation of [**3**]NO$_3$ (**a**), formation of halide-free[Ru(MeOH)(nioxime)(*p*-cymene)]$^{2+}$ and subsequent deprotonation/dimerization (**b**).

2.3. Catalytic activity in the hydrogenation/*N*-methylation of nitroarenes.

The catalytic performances of Ru(II)-dioxime complexes [**1-7**]$^+$ in the reduction/*N*-methylation of nitroarenes were evaluated by GC-FID using nitrobenzene (**a1**) as model compound and methanol as both reductive agent and C$_1$ alkylating source (Table 2). In a preliminary experiment performed using 5 mol% of [**3**]NO$_3$ as catalyst in presence of 1 eq. of potassium *tert*-butoxide (^{t}BuOK) at 100°C for 24 h under nitrogen, we found a conversion of 50 % with a 50 % selectivity to the desired *N*-methylaniline (**b1**) and 50 % to aniline (**c1**) (entry 1). Notably, no trace of *N,N*-dimethyl aniline was detected. The presence of air negatively affected the catalytic performance of [**3**]NO$_3$, reducing the conversion to 34 % and the selectivity for **b1** to 28 % (entry 2). To optimize the reaction conditions for [**3**]NO$_3$, the effect of temperature, reaction time, catalytic loading and base was evaluated. Gratifyingly, the temperature increase from 100°C to 130°C gave full conversion of **a1** and rose the selectivity up to 96 %for **b1** (entry 3). Working at this temperature, it was possible to shorten the reaction time to 18 h without loss of conversion or selectivity (entry 4). However, a significant decrease in the yield of **b1** was observed with shorter reaction times (entry 5). The amount of catalyst could be reduced to 4 mol% without changes in the reaction outcome (98 % conversion, 96 % **b1**, entry 6). On the other hand, a furtherdecrease of the catalytic loading to 3 and

2 mol% produced a negative effect for both conversion and selectivity (entries 7, 8). As expected, the reaction did not occur in the absence of [**3**]NO_3 (entry 9). The catalytic performance of [**3**]NO_3 was significantly affected by the type and amount of base added to the reaction media. The conversion is strongly dependent on the strength of the base (1 eq. respect to**a1**), *i.e.* following the order Cs_2CO_3 (64 %) < $NaOCH_3$ (71 %) < KOH (78 %)<^{t}BuOK (> 99 %) (entries 10-12 vs 6). The reduction of the amount of ^{t}BuOK from 1 to 0.5 eq. had a negative impact on the reaction efficiency, with an important drop in both conversion (75 %) and selectivity (88 %) (entry 13). The absence of a base as co-reactant further decreased the reaction efficiency (entry 14). Note that stoichiometric amounts of base are routinely used to assist the catalytic *N*-methylation of amines or the reduction/*N*-methylation of nitroarenes (see *Introduction*). An additional test employing a catalytic amount of ^{t}BuOK and 3Å molecular sieves gave a very low conversion (entry 15). Therefore, the consumption of ^{t}BuOK by the water generated during $PhNO_2$ hydrogenation and $PhNH_2$ methylation (Scheme 1) does not appear to affect the catalytic process.

Hence, the optimized reaction conditions are [nitroarene]= 0.5 M, 4 mol% of catalytic precursor, 1 eq. of ^{t}BuOK, 130°C for 18h. To distinguish truly homogeneous molecular catalysis from nanoparticle metal catalysis we performed the mercury poisoning test.[8b,8c,8f,35] We observed no significant difference in the catalytic results under optimized conditions in the presence of Hg (entry 16), suggesting a homogeneous nature of the catalytic system. Notably, inthe optimized conditions, the reaction selectively provides *N*-methylaniline and other theoretically possible by-products,such as nitrosobenzene, azobenzene, or azoxybenzene, were not detected, highlighting the excellent selectivity of this procedure.

Table 2. Optimization of the *N*-methylation of nitrobenzene with methanol mediated by [**3**]NO_3.[a]

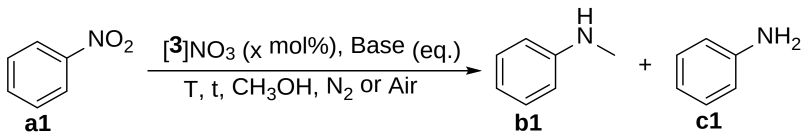

Entry	[3]NO_3 (mol%)	T(°C)	t (h)	Base(eq.)[b]	Conv. (%)[c]	Selectivity (%)[d]	
						b1	c1
1	5	100	24	^{t}BuOK (1.0)	50	50	50
2[e]	5	100	24	^{t}BuOK (1.0)	34	28	72
3	5	130	24	^{t}BuOK (1.0)	>99	96	4
4	5	130	18	^{t}BuOK (1.0)	>99	95	4
5	5	130	10	^{t}BuOK (1.0)	81	72	28
6	4	130	18	^{t}BuOK (1.0)	98	96	4
7	3	130	18	^{t}BuOK (1.0)	90	90	10
8	2	130	18	^{t}BuOK (1.0)	85	93	7
9	-	130	18	^{t}BuOK (1.0)	0	-	-
10	4	130	18	Cs_2CO_3 (1.0)	64	92	8
11	4	130	18	$NaOCH_3$ (1.0)	71	89	11
12	4	130	18	KOH (1.0)	78	94	6
13	4	130	18	^{t}BuOK (0.5)	75	88	12
14	4	130	18	-	53	41	59
15[f]	4	130	18	^{t}BuOK (0.04)	64	58	42
16[g]	4	130	18	^{t}BuOK (1.0)	94	90	10

[a] Reaction conditions: nitrobenzene (0.5 mmol), catalyst [**3**]NO_3 (mol%), base (eq.) in methanol (1 mL). [b] Equivalents calculated on the mol. of nitrobenzene. [c] Conversion based on the consumption of nitrobenzene, determined by GC-FID using mesitylene as an internal standard.[d] Selectivity determined by GC-FID using mesitylene as an internal standard. [e]Reaction carried out under air. [f]Reaction performed in the presence of 3Å molecular sieves.[g] Reaction performed in the presence of 1.5 g of Hg (7.5 mmol, 378 eq.).

Once identified the best conditions, we directed our attention to comparing the catalytic performances of the dioxime-based compounds [**1**-**7**]$^+$ and selected Ru complexes in the benchmark reaction (see Table 3 for an overview of the compounds). Table 3 shows a significant variability in catalysts activity, with important differencesin the selectivity towards the *N*-methylation product. As previously reported by Natte and co-workers,[12c] $RuCl_3·nH_2O$ catalyzed the complete conversion of nitrobenzene. However, at this low catalyst loading, this activity is not accompanied by an acceptable degree of selectivity, resulting in a 41/59 mixture of aniline/*N*-methylaniline (entry 1). The η^6-coordination of an arene, in $[RuCl_2(arene)]_2$ complexes (**D1**, **D3**, **D4**), brings a slight improvement in selectivity with amounts of *N*-methylaniline ranging from 63 to 67 % (entries 2,4,5). Interestingly, the activity of these complexes strictly depends on the coordinated arene. In fact, **D1** (with *p*-cymene, entry 2) provided quantitative conversion of **a1**, but for **D3** (with hexamethylbenzene, entry 4) and **D4** (with mesitylene, entry 5) a clear decrease of the activity wasdetected (84 % and 70 % conversion, respectively). These differences might be due to the relative stability of the metal-arene bond[36] and its possible relation with the pre-catalyst activation step (*vide infra*). The coordinatedhalide has also a relevant impact in the catalytic performances of the η^6-arene Ru dimers: the iodide complex **D2** provided 14% less *N*-methylaniline then its chlorido counterpart **D1** (entry 3 vs 2). In all catalytic cycles where Ru is responsible for dehydrogenation/hydrogenation of substrates, the presence of hydrides is invoked. For this reason, the hydride-bridged dimer **D5**, formal derivative of **D1** with a Cl^- substituted by H^-, was tested as catalyst. **D5** is slightly less active than its tetrachloride counterpart (entry 6 vs. 2) while retaining a similar selectivity. Probably, both species provide a similar active intermediate but the hydride is less robust and decomposes more easily.

Cationic Ru(II) dioxime complexes showed in general a great improvement of the catalytic performances with respect to their starting materials (entries 7-13). In fact, [**1**-**5**]$^+$ and [**7**]$^+$ demonstrated high activities (91 to 99 % conversion), comparable with $RuCl_3 \cdot nH_2O$ or [$RuCl_2$(*p*-cymene)]$_2$ (**D1**), but also excellent selectivity values toward *N*-methylaniline (80-96 % vs. 52-67 % for the halido-bridged dimers). To evaluate the specific contribution of the dioxime substituents, the catalytic properties of [RuCl(C_6Me_6)(dioxime)]$^+$ complexes can be compared. Aliphatic substituents such as methyl- or cyclohexyl- (in [**4**]NO_3 and [**5**]NO_3, respectively) gave rise to very active and selective catalysts (entries 10 and 11), while the stereoelectronic modifications made by the phenylrings in [**6**]PF_6, significantly decreased both conversion and selectivity (entry 12). The influence of the η^6-arene in the catalytic activity is more limited for the dimethylglyoxime ([**1**]$^+$*vs* [**4**]$^+$) or nioxime complexes ([**2**]$^+$*vs* [**5**]$^+$*vs* [**7**]$^+$) than for the respective dimers (**D1**, **D3** and **D4**). For nioxime/*p*-cymene complexes, the presence of the iodido (in [**3**]$^+$) instead of the chlorido (in [**2**]$^+$)

significantly increased the catalytic properties, especially the selectivity to **b1** that rises from 87 % to a remarkable 96% (entry 9 vs 8). Interestingly, the opposite effect was observed for the diruthenium precursors (*vide supra*). Overall, [**3**]NO_3 offers the best catalytic performance among the dioxime complexes and was selected for further investigations (see below).

As showed above, Ru-dioxime complexes are easily deprotonated and the strong basic reaction conditions suggest the *in-situ* formation of the dioximato complexes. Nevertheless, a drastic drop in conversion and selectivity was foundwhen the isolated oxime-oximato complexes $\mathbf{2}^{\mathbf{-H}}$ and $\mathbf{4}^{\mathbf{-H}}$ were tested as catalyst for the methylation of nitrobenzene (entries 14, 15 vs. 8, 10).

Finally, we compared the dioxime based complexes to related ruthenium(II) *p*-cymene compounds containing differenttypes of κ^2-*N*,*N'* ligands. First, the catalytic performance of **N1**, containing a bidentate α-diimine ligand without pendantOH groups, was analyzed. In comparison with [**1-7**]$^+$, **N1** has a similar activity but a 51 % lower selectivity (entry 16). Next, weevaluated the activity of the ethylenediamine compound **N2** and one of the Noyori-Ikariya complexes (**N3**), which represent the state-of-the-art ruthenium catalysts for hydrogenation/dehydrogenation processes.[37] Both compounds contain NH groups,which can be deprotonated in basic conditions,acting as a proton buffers: protonating or deprotonating a substrate at the same time that Ru extracts or releases a hydride. Notably, both **N2** and **N3** resultedless active and extremely less selective than the dioxime compounds (entries 17, 18). Overall, these comparisons clearly point to a crucial role played by the dioxime ligand forthe transfer hydrogenation/*N*-methylation of nitrobenzenewith methanol and are in alignment with the beneficial effects provided by ancillary hydroxyl groups on the catalyst as discussed in the introduction.

Table 3. Comparison of the catalytic properties of Ru complexes in the reduction/*N*-methylation of nitrobenzene with methanol.[a]

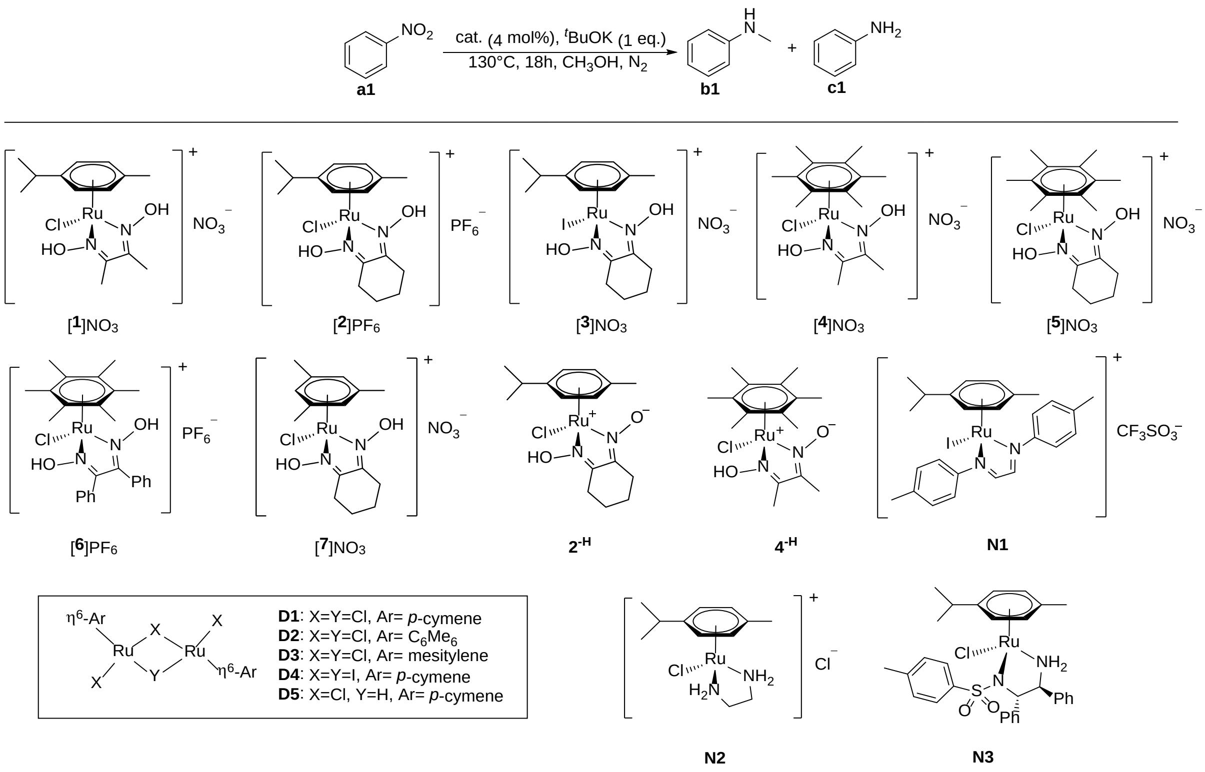

Entry	Catalytic precursor	Conv. (%)[b]	Selectivity (%) [c]	
			b1	**c1**
1	**$RuCl_3·nH_2O$**	>99	59	41
2	**D1**	>99	66	34
3	**D2**	> 99	52	48
4	**D3**	84	63	37
5	**D4**	70	67	33
6	**D5**	89	66	34
7	[**1**]NO_3	91	91	9
8	[**2**]PF_6	95	87	13
9	[**3**]NO_3	98	96	4
10	[**4**]NO_3	95	90	10
11	[**5**]NO_3	> 99	87	13
12	[**6**]PF_6	45	80	20
13	[**7**]NO_3	94	84	16
14	**2^{-H}**	78	51	49
15	**4^{-H}**	58	65	35
16	**N1**	96	55	45
17	**N2**	73	74	26

18	**N3**	86	65	35

[a] Reaction conditions: nitrobenzene (0.5 mmol), catalyst 0.02 mmol for monomers and 0.01 mmol for dimers (4 mol% of Ru), ^{t}BuOK (1 eq.) in methanol (1 mL) at 130°C for 18h. [b] Conversion based on the consumption of nitrobenzene, determined by GC-FID using mesitylene as an internal standard. [c] Selectivity determined by GC-FID using mesitylene as internal standard.

Inspired by the promising results, especially regarding the high activity and selectivity of [**3**]NO_3 towards *N*-methylaniline, we further explored the scope of this catalytic methodology for the *N*-methylation of a series of substituted nitroarenes (Table 4). Interestingly, for all different substrates, we observed the formation of the corresponding *N*-methylaniline with high selectivity, accompanied by a minor amount of aniline. Other potential compounds such as nitrosobenzene, azobenzene or azoxybenzene were never detected. The *N*-methylated anilines were purified by silica chromatography and finally isolated as ammonium salts through treatment with 4 M HCl in dioxane (Figures S50-S66). Good to excellent yields of the corresponding *N*-monomethylated products were obtained with *para* substituted nitroarenes (entries 1-5). Nitrobenzene and *p*-nitrotoluene gave isolated yields of 89 % (entry 1) and 91 % (entry 2) respectively, of the corresponding ammonium salt. Halogen-substituted nitroarenes underwent also a nucleophilic aromatic substitution, resulting in the formation of methoxy-derivatives, as already reported for similar systems (entries 4,5,9).[12b] The presence of a strong electron-donating group as 4-methoxy (entry 3) slightly decreased the reactivity of our catalytic system, while an electron-withdrawing group as 3-CF_3 is well tolerated, giving excellent yield of the corresponding *N*-methylaniline (entry 7). Interestingly, this electron poor substrate, studied for the first time in this work for Ru catalysts, resulted to be much less reactive than the corresponding electron rich nitroarenes for Ir(I)-NHC complexes.[38] In agreement with the results obtained with other homogeneous catalytic systems for the *N*-methylation of nitroarenes, *meta* and *ortho* substituents were less reactive than their *para* analogues (entries 6, 8 and 11).[12b,38] In particular, the presence of *ortho* sterically demanding substituents or an extended aromatic scaffold, as in the case of 1-nitronaphthalene, had a negative influence on both conversion and selectivity (entries 8, 9, 11). An exception in the reactivity of *ortho*-substituted substrates is 1,2-

dinitrobenzene, which was efficiently converted to *N*-methyl-2-nitroaniline (entry 10). This peculiar substrate, containing two reducible/methylable nitrogroups, could provide up to five different products (nitro/NH_2, nitro/*N*-methyl, NH_2/NH_2, NH_2/*N*-methyl, *N*-methyl/*N*-methyl), but only the compound of transfer hydrogenation/methylation of a single NO_2 group was obtained (together with a 10 % of 2-nitroaniline).

Table 4. Reduction/*N*-methylation of a series of nitroarenes with methanol catalyzed by [**3**]NO_3.[a]

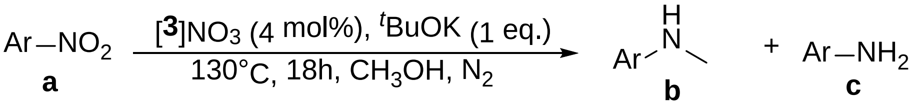

Entry	Substrate	Conv. (%)[b]	Selectivity (%)[c]	
			b	c
1	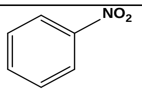	98	96(89)[d]	4
2	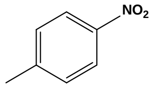	>99	96(91)[d]	4
3	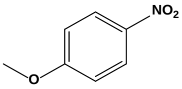	87	80(65)[d]	20
4[e]	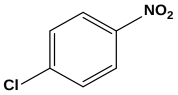	>99[e]	99[f]	/
5[e]	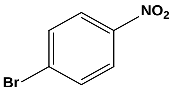	92[e]	99[g]	/
6	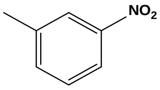	96	85(78)[d]	15
7	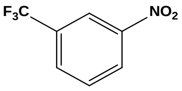	95	92(82)[d]	8
8	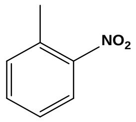	96	70(64)[d]	30
9[e]	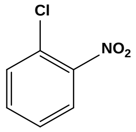	97	87[h]	13

10	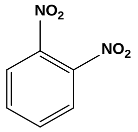	97[g]	90[i](84) [d]	10[j]
11	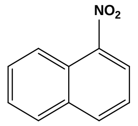	74	79(52) [d]	21

[a] Reaction conditions: nitroarene (0.5 mmol), [**3**]NO_3(4 mol%), ^{t}BuOK (1 eq.) in methanol (1 mL) at 130°C for 18h. [b] Conversion based on the consumption of nitrobenzene, determined by GC-FID using mesitylene as an internal standard. [c] Selectivity determined by GC-FID using mesitylene as internal standard.[d] Isolated yield of ammonium salt after treatment with 4 M HCl in dioxane. [e] Halogen was partially substituted by a methoxy group. [f]88% of 4-methoxy-*N*-methylaniline and 11% of 4-chloro-*N*-methylaniline (not isolated). [g] 94% of 4-methoxy-*N*-methylaniline and 3% of 4-bromo-*N*-methylaniline (not isolated). [h]57% of 2-methoxy-*N*-methylaniline and 30% of 2-chloro-*N*-methylaniline (not isolated). [i]Amount of 2-nitro-*N*-methylaniline. [j] Amount of 2-nitroaniline.

2.4. Mechanistic insights: organic intermediates.

According to the literature, the catalytic transfer hydrogenation/*N*-methylation of nitro compounds proceeds through the oxidation of methanol to formaldehyde, with the concomitant formation of M-H species (Scheme 7, green oval).[3a] These metal hydride species then gradually reduce nitroarenes to aniline in a first catalytic cycle, via intermediates such as nitrosobenzene, *N*-hydroxyaniline, azoxybenzene, azobenzene and diphenylhydrazine.[39] This process can occur directly via hydrogenation of *N*-hydroxyaniline (Scheme 7, orange rectangle), or in by an indirect route through the formation of azobenzene originated from the reduction of azoxybenzene generated by the coupling of nitrosobenzene and *N*-hydroxyaniline (Scheme 7, purple dashed rectangle). In the second catalytic cycle, the aniline reacts with *in situ* generated formaldehyde to get the *N*-methyleneaniline (imine), which is finally hydrogenated to *N*-methylaniline.

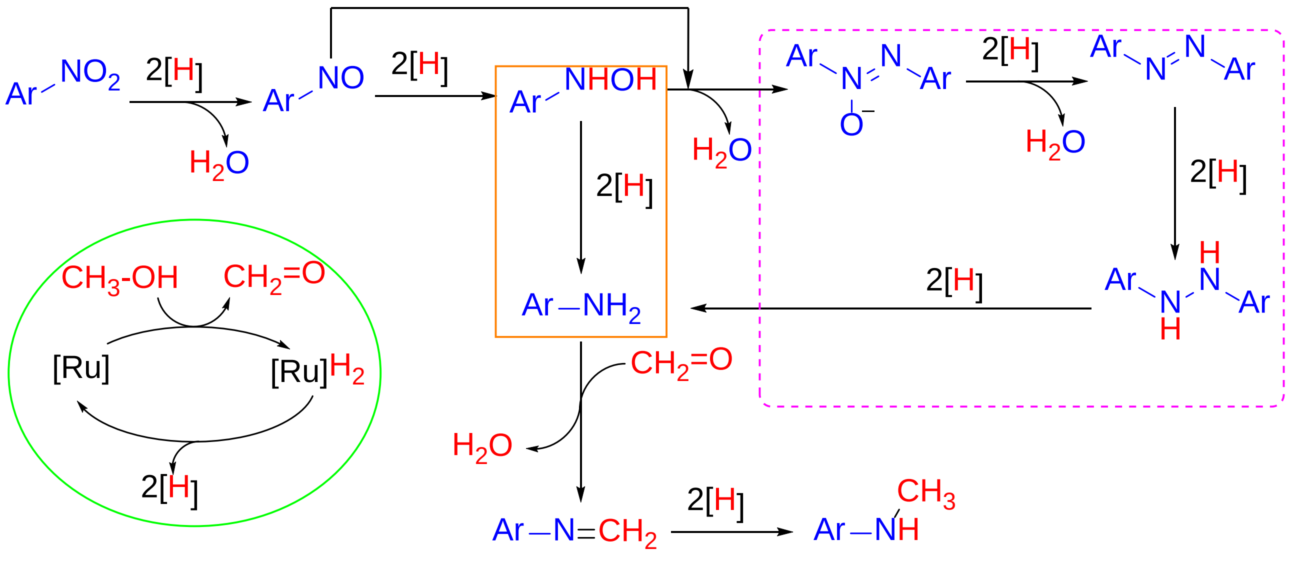

Scheme 7. Overview of the reaction pathways for the Ru-catalyzed transfer hydrogenation / *N*-methylation of nitroarenes with methanol.

Compound [**3**]NO_3 emerged as an effective catalyst for the mono-*N*-methylation of various nitroarenes, exhibiting excellent results in terms of activity and selectivity. Therefore, selected experiments were carried out to gain insights into the reaction mechanism. First, the reaction profile of the reduction/*N*-methylation of nitrobenzene catalyzed by [**3**]NO_3, under the optimized conditions, was monitored by GC-MS to detect the organic intermediates. As shown in Figure 4, after 4 hours a marked decrease in the amount of **a1** was observed (~70 % conversion), along with the formation of ~40 % aniline (**c1**) and ~30 %*N*-methyl aniline (**b1**). Subsequently, the amount of both nitrobenzene and aniline gradually decreased, reaching a final conversion of **a1** of 98 % at 18 h, with a selectivity for **b1** of 96 %. The accumulation of aniline until a maximum of 40 % at 4h, followed by its conversion to **b1** perfectly fits with thetwo reaction cycles with aniline as common species (Scheme 7). Interestingly, neither side products of the reduction of the nitroarene nor the imine were detected at any time interval, suggesting that the conversion of these putative intermediates should be fast.

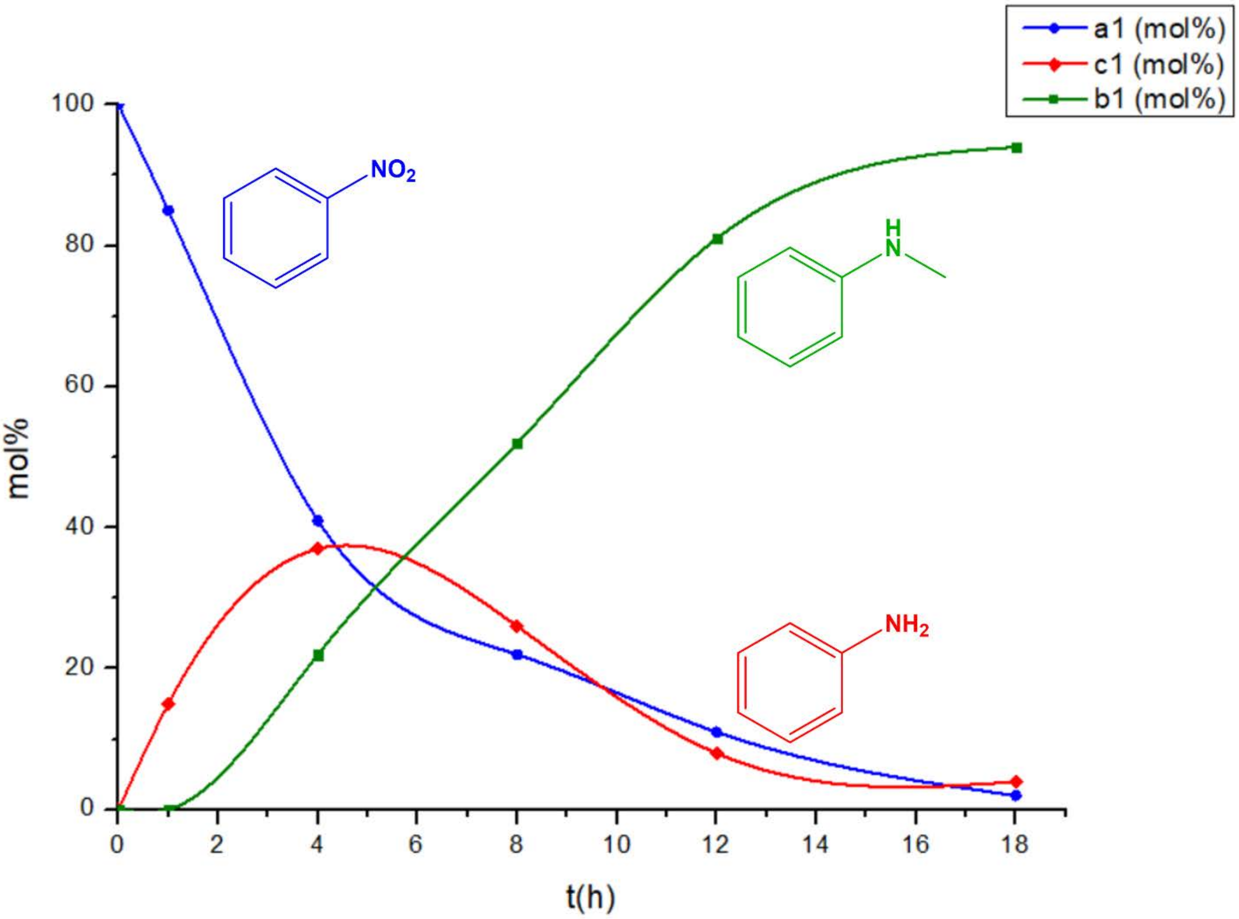

Figure 4. Kinetic investigation on the [**3**]NO_3-catalyzed transfer hydrogenation/*N*-methylation of nitrobenzene with methanol. Reaction conditions: nitrobenzene (0.5 mmol), [**3**]NO_3(4 mol%), ^{t}BuOK (1 eq.) in methanol (1 mL) at 130°C, 0 to 18 h.Data reported in Table S5.

To gain more information about the nitroarene reduction step, the reactivity of azobenzene as starting material was evaluated. M. Beller and co-workers reported that their Pd-based catalytic system was not able to mediate the conversion of azobenzene or azoxybenzene to **b1**, demonstrating that they are not intermediates.[40] On the contrary, with our reaction conditions, [**3**]NO_3 catalyzed the full conversion of azobenzene to *N*-methylaniline (Scheme 8a), proving that both the direct and indirect hydrogenation of nitroarenes could be effective (see Scheme 7).

To shed light into the activation of methanol, the [**3**]NO_3-catalyzed *N*-methylation of nitrobenzene was performed using either methanol-$d_4$or methanol-d_1. The reactions were analyzed by GC-FID, ^{1}H and ^{13}C NMR (Figures S68-S73). Using the optimized reaction conditions, full conversion of **a1** was observed in CD_3OD, with the formation of 87 % of *N*-methylaniline-d_4 (**b1-CD_3**) and 13 % of

N-deuterated aniline **c1-D** (Scheme 8b). On the other hand, the use of CH_3ODled to exclusive incorporation of deuterium in the N−H component (Scheme 8c), with conversion and selectivity comparable to that of the reaction conducted in CH_3OH. These findings confirmed that methanol serves as both carbon and hydrogen source. The small decrease in the selectivity in the experiment with CD_3OD suggests a kinetic isotope effect,which decreases the rate of methylation of the *in situ* generated aniline.

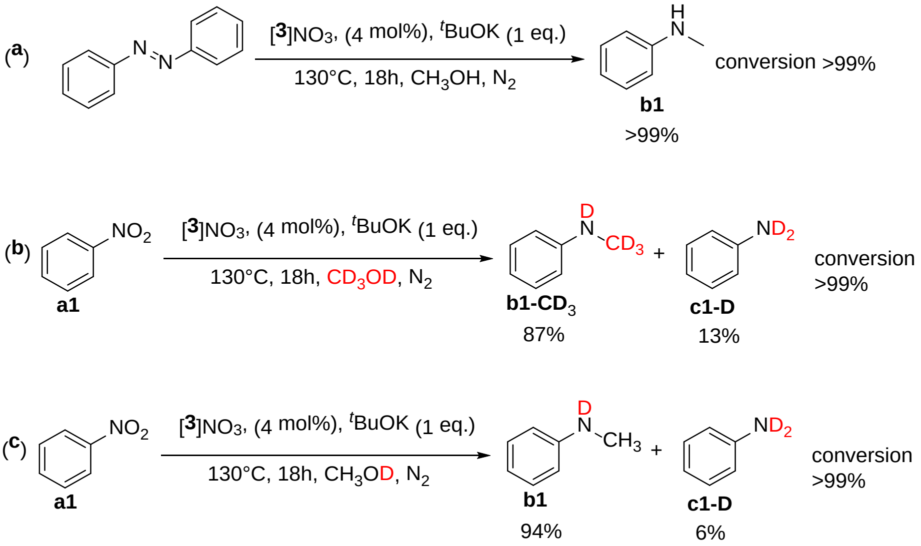

Scheme 8. Control experiments: reduction/*N*-methylation of azobenzene(**a**), reduction/*N*-methylation of **a1** with CD_3OD(**b**), reduction/*N*-methylation of **a1** with CH_3OD(**c**).

To better understand the origin of the high selectivity observed with $[\mathbf{3}]^+$- and with the other dioxime complexes as well - we thought to isolate the nitrobenzene hydrogenation and the aniline methylation steps, analyzing and comparing in both reactions, the catalytic performances of three selected complexes, *i.e.*, the dimer **D1**, the ethylenediamine derivative **N2** and $[\mathbf{3}]NO_3$. To avoid the formation of imines or *N*-alkylated anilines, isopropyl alcohol was selected as H_2source in the reduction of nitrobenzene. The three complexes equally performed in this first step, full converting the nitrobenzene to aniline without detection of any nitro-reduction sideproductsafter 18 h (Scheme 9, red rectangle). On the other hand, a clear difference between the dioxime complex $[\mathbf{3}]^+$ and the other two emerged in *N*-methylation of aniline with methanol (Scheme 9, blue rectangle). In fact, both **D1** and **N2** converted less than 40 % of aniline, while the formation of *N*-methyl aniline was quantitative with[**3**]$^+$. These observations highlight the key roleof dioxime ligands in the *N*-methylation step, possibly acting in cooperation with the metal center.

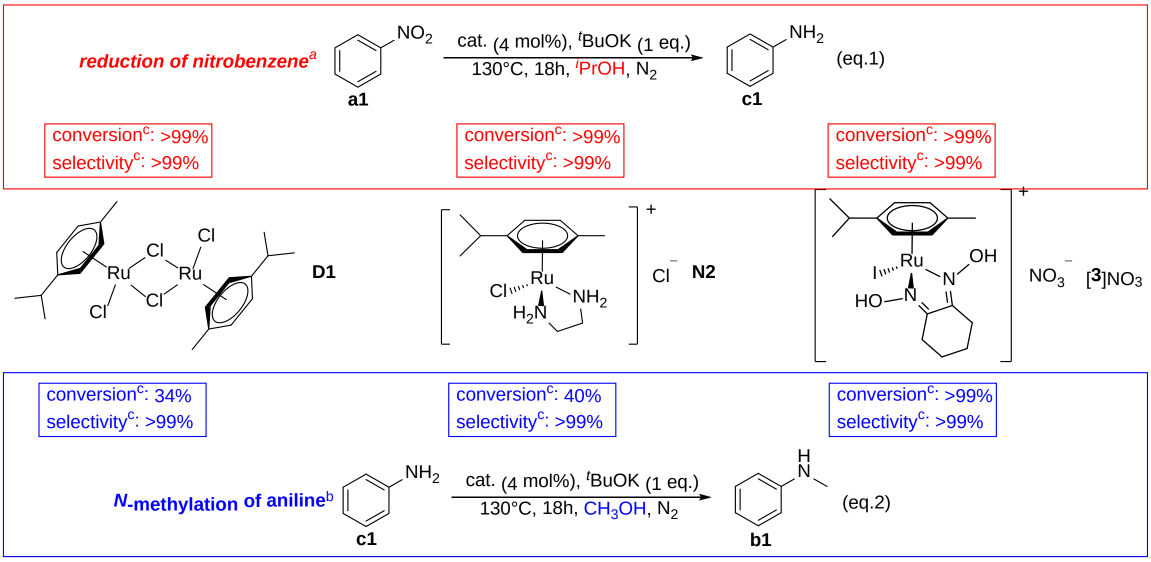

Scheme 9. Comparison of the catalytic properties of selected Ru complexes in the transfer hydrogenation of nitrobenzene with ^{i}PrOH and the reduction/*N*-methylation of nitrobenzene with MeOH. [a] Reaction conditions: nitrobenzene (0.5 mmol), catalyst 0.02 mmol for **N2**, [**3**]NO_3 and 0.01 mmol for **D1**(4 mol% of Ru), ^{t}BuOK (1 eq.) in ^{i}PrOH (1 mL) at 130°C for 18h. [b] Reaction conditions: aniline (0.5 mmol), catalyst 0.02 mmol for **N2**, [**3**]NO_3 and 0.01 mmol for **D1**(4 mol% of Ru), ^{t}BuOK (1 eq.) in MeOH (1 mL) at 130°C for 18h. [c] Conversion and selectivity based on the consumption of nitrobenzene/aniline, determined by GC-FID using mesitylene as an internal standard.

2.5. ESI-MS and ^{1}H NMR studies under catalytically-relevant conditions.

Previous ^{1}H NMR and ESI-MSstudies established that [**3**]$^+$is selectively converted into the dioximato complex [RuI(κ^2*N*-{$(CH_2)_2CNO$}$_2$)(η^6-*p*-cymene)]$^-$, [**3**$^{-2H}$]$^-$ by reaction with ^{t}BuOK (2 eq) in MeOH at room temperature. In order to gain insights into the ruthenium species formed under catalytic conditions, NMR and ESI-MS experiments were carried out. The *in situ* formed [**3**$^{-2H}$]$^-$ appears substantially unaffected by a large excess (20 eq.) of ^{t}BuOK, nitrobenzene or aniline (^{1}H NMR, Figure S74). However, heating the methanol solution to refluxin an open vessel,under N_2(T ≈ 65 °C),led to the progressive detachment of *p*-cymene, which became practically quantitative after 20 h. The release of *p*-cymene from [**3**]NO_3 was also checked by GC-MS during the reduction/*N*-methylation of 3-methylnitrobenzene under the optimized conditions (130 °C, 18 h; Figures S75-S76). The ESI-MS spectra collected at different time intervals under catalytic conditions (MeOH, 130°C) showed the progressive disappearance of $[\mathbf{3}^{-2\mathbf{H}}]^{-}$. However, several low-intensity signals ascribed to Ru-containing species appeared,which we could not identify.

It could be reasonably speculated that cleavage of *p*-cymene from $[\mathbf{3}^{-2\mathbf{H}}]^{-}$ initially leads to the tris-methanol complex $[RuI\{(CH_2)_2CNO\}_2(MeOH)_3]^{-}$ (Scheme 9) or a similar species. Despite very few $\{Ru(MeOH)_3\}$ complexes have been reported,[41] related transformations $[Ru(\eta^6\text{-arene})L_3]$ → $[Ru(solv)_3L_3]$ in more coordinating solvents (like DMSO or MeCN) have been described.[42]

Since the catalytic activity of $[\mathbf{3}]^{+}$ collapses when operating at lower temperatures (Table 2), it is reasonable to assume that the thermally-induced breaking of the ruthenium-*p*-cymene bond generates the catalytically active species. This hypothesis could be generalized to all the dioxime complexes $[\mathbf{1}\text{-}\mathbf{7}]^{+}$. As discussed above, the catalytic performances of $[RuCl(nioxime)(\eta^6\text{-arene})]^{+}$ (*p*-cymene: $[\mathbf{2}]^{+}$; C_6Me_6: $[\mathbf{5}]^{+}$, mesitylene: $[\mathbf{7}]^{+}$) are indeed rather similar (Table 3). In fact, under equal conditions (refluxing MeOH with excess ^{t}BuOK and aniline), also the more robust hexamethylbenzene ligand dissociated from the *in situ* formed dioximato complex $[\mathbf{5}^{-2\mathbf{H}}]^{-}$ (^{1}H NMR).

Arene ligands in ruthenium(II) complexes are often assumed or proved to be spectators in catalytic cycles, as in the Noyori-Ikariya catalyzed transfer hydrogenations.[43] Nevertheless, as in the present study, several cases have been documented where the dissociation of the arene ligand from Ru(II) complexes under catalytic conditions represents the *activation* step of the pre-catalyst.[44]

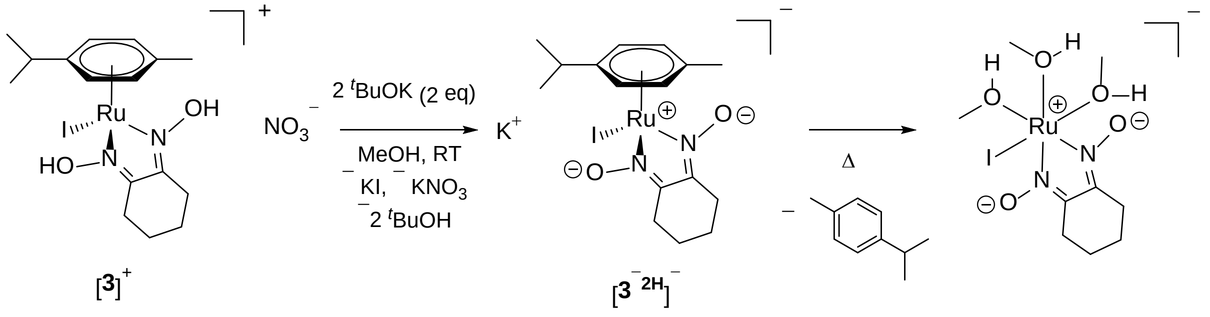

Scheme 9. Possible activation route of the most performing catalytic precursor $[\mathbf{3}]NO_3$: *in situ* bis-deprotonationfollowed by*p*-cymene displacement.

3. Conclusions.

Starting from commercial dioxime ligands, seven unprecedented piano-stool ruthenium(II) complexes featuring different η^6-arene and halide ligands were isolated as nitrate or hexafluorophosphate salts in 77-97 % yields. Three zwitterionic oxime-oximato complexes were prepared by mono-deprotonation of the coordinated dioxime. Crystal structures of both cationic and neutral complexes wereelucidated, representing one of the very few X-Ray studies on dioxime complexes of ruthenium.[25] Under optimized conditions (MeOH, ^{t}BuOK, 130 °C, 18 h), the dioxime complexes showed in general an excellent conversion (91-99 %) and selectivity (80-96 %) in the one-pot transfer hydrogenation and *N*-methylation of nitrobenzene at a low catalyst loading (4 mol%). Comparison of the catalytic performance with other ruthenium(II) arene complexes, including the well-known Noyori-Ikariya's catalyst, emphasized the crucial role played by the dioxime ligand in the hydrogen borrowing step (*N*-methylation of aniline). The most performing compound, [RuI(nioxime)(*p*-cymene)]NO_3, [**3**]NO_3, was also effective in the tandem reduction/*N*-monomethylation of a range of aromatic nitrocompounds. A time-profile analysis and deuterium labeling experiments of the model system (nitrobenzene/[**3**]NO_3) allowed to detect aniline as the only reaction intermediate and to corroborate the role of methanol as H_2 donor and alkylating agent. Additional experiments with [**3**]NO_3 indicated the homogeneous nature of the catalytic system and the thermal dissociation of the *p*-cymene ligand as a plausible activation step of the pre-catalyst.

Overall, the ruthenium(II) arene dioxime complexes herein described are effective catalysts for the tandem reduction/*N*-methylation of nitroarenes, thus encouraging the application of this easily available and tunable class of compounds for other borrowing hydrogen processes. Furthermore, our results suggest, to the broader inorganic chemistry community, the opportunity to include the overlooked dioximes in the panel of ligands for catalyst development.

4. Experimental section.

4.1. General experimental details.

All reagents and solvents were obtained from Alfa Aesar, Sigma Aldrich or TCI Europe and were used without further purifications. Compounds [RuI$_2$(η^6-*p*-cymene)]$_2$(**D2**)[45] and [RuCl(η^6-*p*-cymene)(κ^2*N*-{HCN(4-C$_6$H$_4$CH$_3$)}$_2$)]CF$_3$SO$_3$ (**N1**)[46] were prepared according to literature methods. New or optimized proceduresfor the previously-reported compounds[RuCl$_2$(η^6-*p*-cymene)]$_2$ (**D1**),[36,47] [RuCl$_2$(η^6-C$_6$Me$_6$)]$_2$ (**D3**)[48] [RuCl$_2$(η^6-1,3,5-C$_6$H$_3$Me$_3$)]$_2$(**D4**),[49] [Ru$_2$Cl$_2$(μ-Cl)(μ-H)(η^6-*p*-cymene)$_2$], (**D5**)[47,49,50] [RuCl{κ^2*N*-H$_2$NCH$_2$CH$_2$NH$_2$}(η^6-*p*-cymene)]Cl, (**N2**)[51] and [RuCl{κ^2*N*-(*1S*,*2S*)-H$_2$NC(Ph)C(Ph)NSO$_2$(*p*-C$_6$H$_4$CH$_3$)}(η^6-*p*-cymene)], (**N3**)[43,52] are described in the ESI. Where specified, the reactions were carried out under N$_2$ using standard Schlenk techniques. Anhydrous THF was obtained from SPS 5 solvent purifier (MBraun); MeOH was distilled over CaH$_2$ and stored over 3Å MS. Otherwise, preparations and manipulations were carried out in air with common laboratory glassware.All the complexes were isolated as air-stable powders that were maintained under N$_2$ for long time storage as a precaution (particularly recommended for [**2**]NO$_3$, [**2**]PF$_6$ and [**6**]NO$_3$). Reaction yields are referred to the isolated, powdered materials.Carbon, hydrogen and nitrogen analyses were performed on a Vario MICRO cube instrument (Elementar). Infrared spectra of solid samples (650-4000 cm^{-1} range) were recorded on a Perkin Elmer Spectrum One FT-IR spectrometer equipped with a UATR sampling accessory. NMR spectra were recorded on a Bruker Avance II DRX400, JEOL YH JNM-ECZ400S or JNM-ECZ500R instruments equipped with broadband probes.Chemical shifts are referenced to the residual solvent peaks (^{1}H, ^{13}C) or to external standard (^{14}N to CH$_3$NO$_2$, ^{35}Cl to 1 M NaCl in D$_2$O).[53] Spectra indicated as CH$_3$OH/C$_6$D$_6$ were recorded in CH$_3$OH solutions using a sealed C$_6$D$_6$ capillary for locking. NMR resonances were assigned with the assistance of ^{1}H-^{13}C *gs*-HSQC and/or *gs*-HMBC correlation experiments. UV-Vis spectra (190-900 nm) were recorded on an Ultraspec 2100 Pro spectrophotometer. IR and UV-Vis spectra were processed with Spectragryph.[54] Conductivity measurements were carried using an XS COND 8 instrument (cell constant = 1.0 cm^{-1})[55] equipped with NT 55 temperature probe (measurements automatically adjusted to 25 °C). KNO$_3$ [Λ_m (MeOH,

$2.7\cdot10^{-3}$ M): 93 $S\cdot cm^2\cdot mol^{-1}$] and $[Bu_4N]Br$ [Λ_m (MeOH, $3.2\cdot10^{-3}$ M): 62 $S\cdot cm^2\cdot mol^{-1}$] were used as a reference compounds.[56] Mass spectrometry measurements were performed on a quadrupole time-of-flight mass spectrometer instrument (Q-TOF) (Xevo G2 QTof; Waters) operated with MassLynx (version 4.1, Waters) software package. The spectra were scanned in the m/z range from 50 to 1200. ESI Z-spray conditions: flow rate 5 μL/min; electrospray capillary voltage: 3.0 kV; source temperature: 100 °C; gas: N_2; gas temperature: 250 °C. The cone voltage was adjusted according to the MassLynx software to 20 and the extraction cone to 2. The argon buffer gas in the T-wave was set at about 0.3 mL/min.Gas chromatography-mass spectrometry measurements were performed by a ThermoFischer Trace 1300 series instrument equipped with a mass spectrometer ThermoFischer ISQ 4000 (230 V) detector, using a J&W HP-5 30 m × 0.32 mm × 0.25 μm film thickness fused silica column and chromatography grade helium as carrier gas.

4.2. Synthesis and characterization of dioxime andoxime-oximato complexes.

Procedure A ([**1**-**7**]NO_3). An orange suspension of $[RuCl_2(\eta^6\text{-arene})]_2$ (50-200 mg; arene = *p*-cymene, C_6Me_6, 1,3,5-$C_6H_3Me_3$) and $AgNO_3$ (2.0 equivalents) in MeCN (*ca*. 5 mL) was stirred at room temperature for 1 h (3.5 h for arene = 1,3,5-$C_6H_3Me_3$) under protection from the light. The resulting mixture (yellow/orange solution + colorless solid) was filtered over celite and treated with the selected dioxime (2.0 equivalents).The solution was stirred at room temperature (reflux temperature for arene = 1,3,5-$C_6H_3Me_3$) for 3 h and the conversion was checked by ^1H NMR (CD_3OD).Following an appropriate filtration step over celite, volatiles were removed under vacuum. The resulting solid was triturated in Et_2O (Et_2O/MeCN 6:1 *v*/*v*for [**4**]NO_3 and [**6**]NO_3) and the suspension was filtered.The solid was washed with Et_2O, hexane and dried under vacuum (40 °C).*Note*: the presence of even a slight excess of $AgNO_3$ leads to formation of by-products, among which free *p*-cymene; it is important to use stochiometric amounts.

Procedure B ([**2**,**3**]NO_3). An orange suspension of $[RuX_2(\eta^6\text{-}p\text{-cymene})]_2$ (54-160 mg, X = Cl, I) and $AgNO_3$ (2.0 equivalents) in MeOH (5-8mL) was stirred at room temperature for 1.5 h under protection from the light. The suspension (X = Cl: yellow-orange solution + colorless solid; X = I: red-brown solution + pale yellow solid) was filtered over celite and the filtrate was treated with nioxime (2.0 equivalents). The mixture was stirred at room temperature for 1.5 h affording a clear red (X = I) or orange (X = Cl) solution. Conversion was checked by ^{1}H NMR (CD_3OD) then volatiles were removed under vacuum. The residue was dissolved in CH_2Cl_2 (X = I: a few drops of MeOH were added to assist solubilization) and filtered over celite. The filtrate was taken to dryness under vacuum and the resulting foamy solid was triturated in Et_2O/hexane 1:1 *v*/*v*. The suspension was filtered; the solid was washed with Et_2O/hexane 1:1 *v*/*v*, hexane and dried under vacuum (40 °C).

Alternative preparations involving the use of MeCN in both reaction steps (as in procedure A) or MeCN in the first step and MeOH in the second step led to the isolation of a more brownish solid containing [**2**,**3**]NO_3 and minor amounts of non-arene nioxime complexes. Coherently, the presence of free *p*-cymene was assessed in the final reaction mixture.

Procedure C ([**2,6**]PF_6). A suspension of [$RuCl_2(\eta^6$-arene)]$_2$ (33-70 mg; arene = *p*-cymene, C_6Me_6) and the selected dioxime (2.0 equivalents) in EtOH (6 mL) was stirred at room temperature for 1 h, then treated with KPF_6 (*ca*. 2.2 equivalents). After 2 h, the suspension (yellow-orange solution + colorless solid) was filtered over celite and the filtrate was taken to dryness under vacuum. The residue was dissolved in CH_2Cl_2 and filtered over celite. Volatiles were removed from the filtrate solution andthe resulting solid was triturated in Et_2O. The suspension was filtered, the solidwas washed with Et_2O, hexane and dried under vacuum (40 °C).

Procedure D (**2-4**$^{\mathbf{-H}}$). A suspension of [$RuX_2(\eta^6$-arene)]$_2$ (55-70 mg; X= Cl, I; arene = *p*-cymene, C_6Me_6) and the selected dioxime (2.0 equivalents) in MeOH (4 mL) was stirred at room temperature for 1.5 h, then treated with $NaHCO_3$ (2.0 equivalents) and stirred for 2 h. A yellow (X = Cl) or yellow-brown (X = I) solution formed within few minutes. For **2**$^{\mathbf{-H}}$ and **4**$^{\mathbf{-H}}$:volatiles were removed under vacuum and the residue was suspended in CH_2Cl_2. For **3**$^{\mathbf{-H}}$: the final mixture was diluted with MeOH. The suspension was filtered over celite and the filtrate was taken to dryness under vacuum. The resulting solid was triturated in Et_2O and filtered. The solid was washed with Et_2O, hexane and dried under vacuum (40 °C).

[RuCl(κ^2*N*-{$CH_3C=NOH$}$_2$)(η^6-*p*-cymene)]NO_3, [1]NO_3 (Chart 1).

Chart 1. Structure of [**1**]$^+$ (numbering refers to carbon atoms).

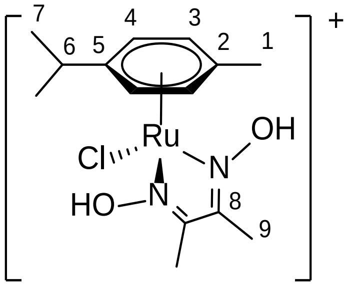

Prepared from [$RuCl_2$(η^6-*p*-cimene)]$_2$ (54 mg, 0.088 mmol, 1 eq), $AgNO_3$ (30 mg, 0.18 mmol) and dimethylglyoxime (20 mg, 0.18 mmol), according to procedure A.Final reaction mixture: yellow-orange solution; filtered over celite.Orange solid, yield: 62 mg, 77 %. Soluble in MeOH, MeCN, insoluble in Et_2O, toluene. Anal. Calcd. for $C_{14}H_{22}ClN_3O_5Ru$: C, 37.46; H, 4.94; N, 9.36; Found: C, 36.3; H, 4.47; N, 8.91. IR (solid state): $\tilde{\upsilon}$/cm^{-1} = 3300-3100m-br (OH), 3071-3057w-br, 2971w, 2925w, 2730-2701w, 1464m-sh, 1435m-sh, 1389m, 1364m, 1323m, 1254s-br (NO_3), 1193s, 1162w-sh, 1118w, 1064s (NO), 1035m, 1006s, 875w, 824w, 804w, 720w, 674w.^{1}H NMR (CD_3OD): δ/ppm = 6.06 (d, $^3J_{HH}$ = 6.4 Hz, 2H, C^4H), 5.69 (d, $^3J_{HH}$ = 6.4 Hz, 2H, C^3H), 2.71 (hept, $^3J_{HH}$ = 7.0 Hz, 1H, C^6H), 2.32 (s, 6H, C^9H), 2.28 (s, 3H, C^1H), 1.18 (d, $^3J_{HH}$ = 6.9 Hz, 6H, C^7H). ^{13}C{^{1}H} NMR (CD_3OD): δ/ppm = 161.0 (C^8), 109.9 (C^5), 107.0 (C^2), 88.9 (C^4), 85.7 (C^3), 32.6 (C^6), 22.4 (C^7), 19.3 (C^1), 13.6 (C^9). ^{14}N NMR (CD_3OD): δ (ppm) = − 3.7 ($\Delta\nu_{1/2}$ = 21 Hz, NO_3^-).

[RuCl(κ^2*N*-{$CH_2CH_2C=NOH$}$_2$)(η^6-*p*-cymene)]X, [2]X (X = NO_3, PF_6; Chart 2).

Chart 2. Structure of [**2**]$^+$ (numbering refers to carbon atoms).

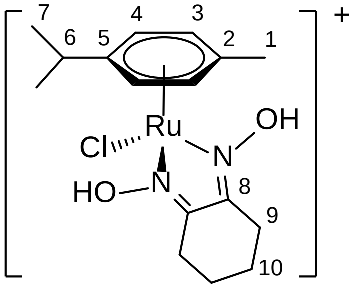

[2]PF₆.Prepared from [RuCl$_2$(η^6-*p*-cimene)]$_2$ (70 mg, 0.114 mmol), nioxime (33 mg, 0.23mmol) and KPF$_6$ (45 mg, 0.24 mmol), according to procedure C. Ochre yellow-orange solid, yield: 104 mg, 82 %. Alternatively prepared according to procedure A, using NH$_4$PF$_6$ (89 mg, 0.545 mmol) in place of AgNO$_3$,[RuCl$_2$(η^6-*p*-cimene)]$_2$ (165 mg, 0.269 mmol) and nioxime (78 mg, 0.549 mmol). Yield: 256 mg, 85 %. Stored under N$_2$ (partially decomposed to a dark brown solid after several months when stored in air). Soluble in MeCN, acetone, water, less soluble in CH$_2$Cl$_2$, poorly soluble in CHCl$_3$,insoluble in Et$_2$O, toluene.Anal. Calcd. For C$_{16}$H$_{24}$ClF$_6$N$_2$O$_2$PRu: C, 34.45, H, 4.34, N, 5.02; Found: C, 33.92, H, 4.16, N, 5.01.IR (solid state): $\tilde{\upsilon}$/cm^{-1} = 3640-3600w (OH), 3563w (OH), 3433w-br (OH), 2436w, 3100m-br, 2097m, 2949w,2878w, 1546w, 1508w, 1470m, 1461m, 1456m, 1432m, 1425m, 1387m-sh, 1396s, 1309s, 1258w, 1242w, 1189m, 1167w, 1116w, 1094w, 1039s (NO), 1009w, 972m, 923w, 908w,838vs (PF$_6$), 817vs-sh, 786s, 739m, 729s, 680w.^{1}HNMR (acetone-d$_6$): δ/ppm = 6.38 (d, $^3J_{HH}$ = 6.0 Hz, C^{4}H), 5.91 (d, $^3J_{HH}$ = 6.0 Hz, C^{3}H), 3.00–2.79 (m, 5H, C^{6}H + C^{9}H), 2.27 (s, 3H, C^{1}H), 1.77–1.60 (m, 4H, C^{10}H), 1.21 (d, $^3J_{HH}$= 6.9 Hz, 6H, C^{7}H); N(OH) signals were not detected (rapid H/D exchange with residual water). ^{1}HNMR (CD$_3$OD): δ/ppm = 6.07 (d, $^3J_{HH}$ = 6.3 Hz, 2H, C^{4}H), 5.69 (d, $^3J_{HH}$ = 6.3 Hz, 2H, C^{3}H), 2.94–2.78 (m, 4H, C^{9}H), 2.72 (hept, $^3J_{HH}$ = 6.9 Hz, 1H, C^{6}H), 2.28 (s, 3H, C^{1}H), 1.73–1.62 (m, 4H, C^{10}H), 1.18 (d, $^3J_{HH}$ = 6.9 Hz, 6H, C^{7}H). No changes in the ^{1}H NMR spectrum were observed after 14h at room temperature. ^{13}C{^{1}H}NMR (CD$_3$OD): δ/ppm = 161.0 (C^8), 110.0 (C^2), 106.9 (C^5), 88.7 (C^4), 85.4 (C^3), 32.7 (C^6), 27.2 (C^9), 22.4 (C^7), 21.4 (C^{10}), 19.3 (C^1). ^{19}FNMR (CD$_3$OD): δ/ppm = − 74.8 (d, $^1J_{FP}$ = 708 Hz, PF$_6^-$). ^{31}PNMR (CD$_3$OD): δ/ppm = − 144.6 (hept, $^1J_{FP}$ = 708 Hz, PF$_6^-$).

[2]NO₃.Prepared from [RuCl$_2$(η^6-*p*-cimene)]$_2$ (54 mg, 0.088 mmol), AgNO$_3$ (30 mg, 0.18 mmol) and nioxime (26 mg, 0.18 mmol), according to procedure B.Ochre yellow-orange solid, yield: 67 mg, 67 %.Stored under N_2. Soluble in acetone, MeOH, CH_2Cl_2; insoluble in Et_2O, hexane. Anal. Calcd. For: $C_{16}H_{24}ClN_3O_5Ru$: C, 40.47; H, 5.09; N, 8.85. Found: C, 40.33; H, 5.13; N, 8.68.IR (solid state): $\tilde{\upsilon}$/cm^{-1} = 3060w, 2945m, 2873m, 2700w-br, 1472m-sh, 1447m-sh, 1434m, 1417s, 1388s, 1379s, 1363m, 1325m, 1299m-sh, 1262s, 1243s (NO_3), 1184s, 1163s-sh, 1086w, 1072w, 1038m (NO), 1019m-sh, 971s, 909w, 890w, 873w, 823w, 805w, 750w, 713-677w. ^{1}HNMR (CD_3OD or acetone-d_6): identical to the PF_6^- salt. UV-Vis (MeOH, $2.1\cdot10^{-3}$ M): λ_{max}/nm (ε/M$^{-1}\cdot$cm^{-1}) = 243sh ($8\cdot10^3$), 274sh ($6.3\cdot10^3$), 328 ($5.0\cdot10^3$), 390br ($1.9\cdot10^3$). Λ_m (MeOH, $2.1\cdot10^{-3}$ M): 93 S·cm^2·mol^{-1}.

[RuI(κ^2*N*-{CH_2CH_2C=NOH}$_2$)(η^6-*p*-cymene)]NO_3, [3]NO_3 (Chart 3).

Chart 3. Structure of [**3**]$^+$ (numbering refers to carbon atoms).

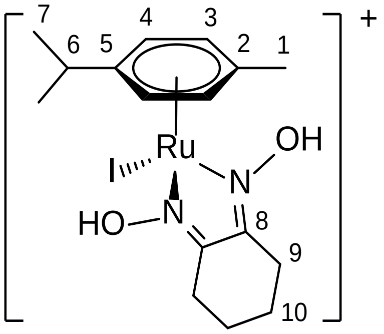

Prepared from [RuI_2(η^6-*p*-cymene)]$_2$ (160 mg, 0.164 mmol), $AgNO_3$ (55.5 mg, 0.327 mmol) and nioxime (47 mg, 0.33 mmol), according to procedure B.Orange-brown solid, yield: 160 mg, 86 %.Soluble in MeOH, MeCN, acetone,water, less soluble in CH_2Cl_2, H_2O, insoluble in Et_2O.X-ray quality needle-like crystals of [**3**]NO_3 were obtained from an EtOH solution layered with a toluene/hexane mixture and settled aside at – 20 °C. Anal. Calcd. for $C_{16}H_{24}IN_3O_5Ru$: C, 33.93; H, 4.27; N, 7.42. Found: C, 33.84; H, 4.35; N, 7.52.IR (solid state): $\tilde{\upsilon}$/cm^{-1} = 3200w-br (OH), 3079w, 2955w, 2931w, 2870w, 2740w-br, 1454m-sh, 1418m-sh, 1388s, 1368s, 1326m-sh, 1270s (NO_3), 1243s, 1186s, 1164s-sh, 1135m-sh, 1113m, 1086m, 1043s (NO), 1019m-sh, 969s, 906w, 879w, 825w, 805w, 789w, 733w, 714w. ^{1}H NMR (CD_3OD): δ/ppm = 5.99 (d, $^3J_{HH}$ = 6.2 Hz, 2H, C^{4}H), 5.65 (d, $^3J_{HH}$ = 6.1 Hz, 2H, C^{3}H), 2.97–2.74 (m, 5H, C^{9}H + C^{6}H), 2.65 (s, 3H, C^{1}H), 1.73–1.56 (m, 4H, $C^{10}H$), 1.20 (d, $^{3}J_{HH}$ = 6.9 Hz, 6H, $C^{7}H$). $^{13}C\{^{1}H\}$ NMR (CD_3OD): δ/ppm = 159.8 (C^{8}), 110.1 (C^{2}), 108.2 (C^{5}), 88.6 (C^{4}), 86.0 (C^{3}), 33.2 (C^{6}), 27.3 (C^{9}), 22.4 (C^{7}), 21.8 (C^{1}), 21.5 (C^{10}).

[RuCl(κ^{2}*N*-{CH_3C=NOH}$_2$)(η^{6}-C_6Me_6)]NO_3, [4]NO_3 (Chart 4).

Chart 4. Structure of [**4**]$^{+}$ (numbering refers to carbon atoms).

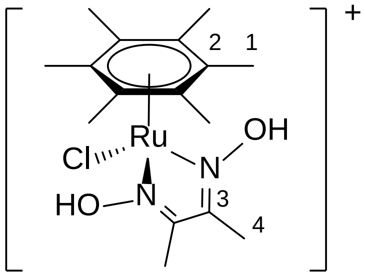

Prepared from [$RuCl_2$(η^{6}-C_6Me_6)]$_2$ (60 mg, 0.090 mmol), $AgNO_3$ (30 mg, 0.18 mmol) and dimethylglyoxime (21 mg, 0.18 mmol), according to procedure A. Final reaction mixture: pale yellow solution and yellow solid; dried under vacuum, dissolved in MeOH and filtered over celite.Yellow solid, yield: 68 mg, 82 %. Soluble in MeOH, water, poorly soluble in MeCN, insoluble in Et_2O. X-ray quality crystals of [**4**]$NO_3\cdot H_2O$ were obtained from an EtOH solution spiked with a drop of 65 % $HNO_{3(aq)}$, layered with Et_2O and settled aside at – 20°C. Anal. Calcd. for $C_{16}H_{26}ClN_3O_5Ru$: C, 40.30; H, 5.50; N, 8.81; Found: C, 40.12; H, 5.68; N, 8.82.IR (solid state): $\tilde{\upsilon}$/cm^{-1} = 3022m-sh (OH), 2297m-sh, 2914m, 2656m-br, 1612w, 1534w, 1416s, 1386s, 1276s (NO_3), 1192s, 1072s (NO), 1039m, 1016m, 998s, 962s, 833w, 826w, 719w, 668w.^{1}HNMR (CD_3OD): δ/ppm = 2.30 (s, 6H, $C^{4}H$), 2.17 (s, 18H, $C^{1}H$). $^{13}C\{^{1}H\}$ NMR (CD_3OD): δ/ppm = 162.3 (C^{3}), 99.7 (C^{2}), 15.8 (C^{1}), 13.7 (C^{4}).UV-Vis (MeOH, $2.1\cdot10^{-3}$ M): λ_{max}/nm (ε/$M^{-1}\cdot cm^{-1}$) = 345 ($4.0\cdot10^{3}$), 403 ($2.9\cdot10^{3}$). Λ_m (MeOH, $2.1\cdot10^{-3}$ M): 102 $S\cdot cm^{2}\cdot mol^{-1}$.

[RuCl(κ^{2}*N*-{CH_2CH_2C=NOH}$_2$)(η^{6}-C_6Me_6)]NO_3, [5]NO_3 (Chart 5).

Chart 5. Structure of [**5**]$^{+}$ (numbering refers to carbon atoms).

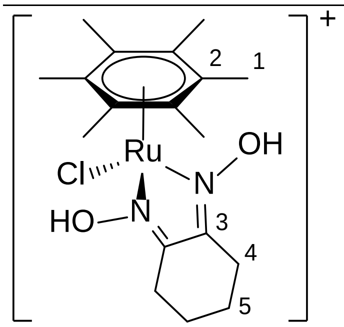

Prepared from $[RuCl_2(\eta^6\text{-}C_6Me_6)]_2$ (99 mg, 0.148 mmol), $AgNO_3$ (50 mg, 0.30 mmol) and nioxime (42 mg, 0.30 mmol), according to procedure A. Final reaction mixture: yellow-orange solution + solid; dried under vacuum, dissolved in MeOH and filtered over celite. Yellow-ochre solid, yield: 144 mg, 97 %.Soluble in MeOH, less soluble in MeCN, poorly soluble in CH_2Cl_2, insoluble in Et_2O, hexane. Anal. Calcd. for $C_{18}H_{28}ClN_3O_5Ru$: C, 42.99; H, 5.61; N, 8.35. Found: C, 43.06; H, 5.45; N, 8.29. IR (solid state): $\tilde{\upsilon}/cm^{-1}$ = 3441w (OH), 3366w (OH), 2945m, 2875w, 2660m-br, 1452m-sh, 1435s-sh, 1393s, 1377s, 1350s-sh, 1315m, 1273s (NO_3), 1256s-sh, 1238s-sh, 1184s, 1165m, 1141m, 1073m, 1031s (NO), 970m, 904m, 866w, 823w, 778w, 731w, 718w.^{1}H (CD_3OD): δ/ppm = 2.98–2.79 (m, 4H, C^4H), 2.19 (s, 18H, C^1H), 1.80–1.58 (m, 4H, C^5H). $^{13}C\{^1H\}$ (CH_3OH/C_6D_6): δ/ppm = 163.4 (C^3), 99.6 (C^2), 27.2 (C^4), 21.2 (C^5), 15.6 (C^1). ^{14}N (CD_3OD): δ/ppm = – 4.3 ($\Delta\nu_{1/2}$ = 20 Hz).

$[RuCl(\kappa^2N\text{-}\{PhC{=}NOH\}_2)(\eta^6\text{-}C_6Me_6)]X$, [6]X (X = NO_3, PF_6; Chart 6).

Chart 6. Structure of [**6**]$^+$ (numbering refers to carbon atoms).

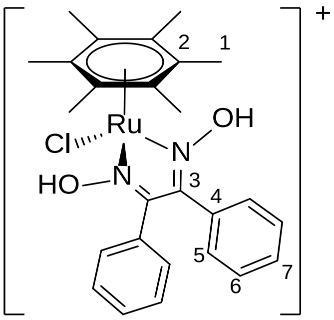

[6]NO$_3$. Prepared from $[RuCl_2(\eta^6\text{-}C_6Me_6)]_2$ (166 mg, 0.248 mmol), $AgNO_3$ (85 mg, 0.50 mmol) and diphenyldioxime (125 mg, 0.518 mmol), according to procedure A. Final reaction mixture: pale yellow solution and orange solid; dried under vacuum, dissolved in MeOH and filtered over celite.

Orange-brown solid, yield: 261 mg, 87 %. Stored under N_2.Soluble in MeOH, poorly soluble in MeCN, insoluble in Et_2O. Anal. Calcd. for $C_{26}H_{30}ClN_3O_5Ru$: C, 51.96; H, 5.03; N, 6.99; Found: C, 51.26; H, 4.88; N, 6.83.IR (solid state): $\tilde{\upsilon}$/cm^{-1} = 3463-3405w-br (OH), 3027w, 2878w-br, 2600w-br, 1433m, 1402s, 1393s, 1353s, 1272s (NO_3), 1247s, 1220s, 1120w, 1089s (NO), 1072m, 1063m, 1038m, 1028m, 1016m, 1001m, 922w, 886m, 847w, 819w, 795w, 774w, 764m, 724s, 694s.^{1}H NMR (CD_3OD): δ/ppm = 7.36–7.24 (m, 6H, C^6H + C^7H), 7.09–7.04 (m, 4H, C^5H), 2.28 (s, 18H, C^1H).$^{13}C\{^1H\}$ NMR (CD_3OD): δ/ppm = 163.6 (C^3), 131.3 (C^7), 130.7 (C^6), 130.1 (C^4), 129.3 (C^5), 101.5 (C^2), 16.0 (C^1). ^{14}N NMR (CD_3OD): δ/ppm = – 5.3 ($\Delta\nu_{1/2}$ = 19 Hz, NO_3).

[6]PF$_6$.Prepared from $[RuCl_2(\eta^6\text{-}C_6Me_6)]_2$ (101 mg, 0.151 mmol), diphenyldioxime (73 mg, 0.30 mmol) and KPF_6 (60 mg, 0.33 mmol), according to procedure C.Orange solid, yield: 176 mg, 85 %. Unlike in the preparation of [**2**]PF_6, no reaction occurs until the addition of KPF_6 (the insoluble $[RuCl_2(\eta^6\text{-}C_6Me_6)]_2$did not react with nioxime). Soluble in MeOH, EtOH, CH_2Cl_2, poorly soluble in Et_2O.Anal. Calcd. For. $C_{26}H_{30}ClN_3O_5Ru$: C, 45.65; H, 4.42; N, 4.10. Found: C, 45.35; H, 4.54; N, 4.03.^{1}H NMR (CD_3OD): δ/ppm = identical to the NO_3^- salt. ^{19}F NMR (CD_3OD): δ/ppm = -74.8 (d, J = 706 Hz).^{19}F NMR (CD_3OD): δ/ppm = − 74.8 (d, $^1J_{FP}$ = 706 Hz, PF_6^-).^{31}P NMR (CD_3OD): δ/ppm = −144.6 (hept, $^1J_{FP}$ = 706 Hz, PF_6^-).

$[RuCl(\kappa^2N\text{-}\{CH_2CH_2C{=}NOH\}_2)(\eta^6\text{-}1,3,5\text{-}C_6H_3Me_3)]NO_3$, [7]$NO_3$(Chart 7).

Chart 7. Structure of [**7**]$^+$ (numbering refers to carbon atoms).

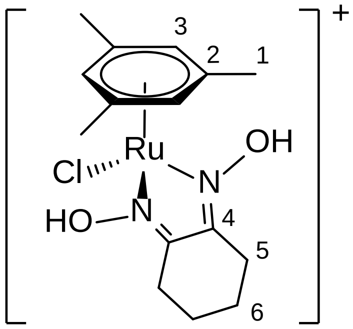

Prepared from $[RuCl_2(\eta^6\text{-}1,3,5\text{-}C_6H_3Me_3)]_2$ (53 mg, 0.090 mmol), $AgNO_3$ (32 mg, 0.19 mmol) and nioxime (27 mg, 0.19 mmol), according to procedure A. Final reaction mixture: brown solution;

dried under vacuum, dissolved in acetone and filtered over celite. Brown solid, yield: 71 mg, 86 %. Soluble in MeOH, acetone; poorly soluble in CH_2Cl_2, insoluble in Et_2O, hexane. Anal. Calcd. for $C_{15}H_{22}ClN_3O_5Ru$: C, 39.09; H, 4.81; N, 9.12. Found: C, 38.95; H, 4.90; N, 9.06.IR (solid state): $\tilde{\upsilon}$/cm^{-1} = 3420w-br (OH), 3078w, 3041w, 2945m, 2870m, 2701w-br, 1881w, 1646w, 1531w, 1452m-sh, 1417s-sh, 1378s, 1323-sh, 1299s-sh, 1272s, 1252s (NO_3), 1186s, 1166m-sh, 1072w, 1033s (NO), 1012w-sh, 989w, 970m, 905w, 887w, 824w, 785w, 732w, 714w. ^{1}H NMR (CD_3OD): δ/ppm = 5.38 (s, 3H, C^{3}H), 2.82 (app. t, $^3J_{HH}$ = 6.5 Hz, 4H, C^{5}H), 2.32 (s, 9H, C^{1}H), 1.79–1.70, 1.68–1.60 (m, 4H, C^{6}H). ^{13}C{^{1}H} NMR (CD_3OD): δ/ppm = 160.6 (C^4), 111.6 (C^2), 81.3 (C^3), 27.1 (C^5), 21.6 (C^6), 19.5 (C^1). ^{14}N NMR (CD_3OD): δ/ppm = – 3.9 ($\Delta\nu_{1/2}$ = 33 Hz).

[RuCl(κ^2*N*-{ONC(CH_2)$_4$CNOH})(η^6-*p*-cymene)], 2^{-H}(Chart 8).

Chart 8. Structure of **2^{-H}** (numbering refers to carbon atoms).

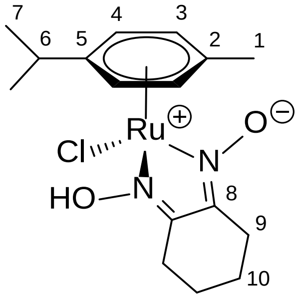

Prepared from [RuCl$_2$(η^6-*p*-cymene)]$_2$ (70 mg, 0.114 mmol), nioxime (33 mg, 0.23 mmol) and $NaHCO_3$ (19 mg, 0.23 mmol), according to procedure D.Yellow-orange solid, yield: 86 mg, 91 %. Soluble in MeOH, CH_2Cl_2, less soluble in acetone, MeCN, scarcely soluble in Et_2O. Anal. Calcd. for $C_{16}H_{23}ClN_2O_2Ru$: C, 46.66; H, 5.63; N, 6.80. Found: C, 45.27; H, 5.35; N, 6.49. IR (solid state): $\tilde{\upsilon}$/cm^{-1} = 3064w, 2959w, 2928w, 2864w, 1595w, 1500w-sh, 1467m, 1449m, 1427m, 1385m, 1300w, 1303m, 1253w, 1228w, 1162s, 1101s (N=O), 1029s (N-O), 999s-sh, 898s, 864m-sh, 798s, 747w.^{1}H NMR (CD_3OD): δ/ppm = 5.75 (d, $^3J_{HH}$ = 6.3 Hz, 2H, C^{4}H), 5.38 (d, $^3J_{HH}$ = 6.2 Hz, 2H, C^{3}H), 2.72 (hept, $^3J_{HH}$ = 6.9 Hz, 1H, C^{6}H), 2.66–2.59 (m, 4H, C^{9}H), 2.20 (s, 3H, C^{1}H), 1.61–1.53 (m, 4H, C^{10}H), 1.15 (d, $^3J_{HH}$ = 6.9 Hz, 6H, C^{7}H). ^{13}C{^{1}H} NMR (CD_3OD): δ/ppm = 165.8 (C^8); 106.5 (C^5), 103.0 (C^2), 89.3 (C^4), 85.9 (C^3), 32.5 (C^6), 26.5 (C^9); 22.50, 22.48 (C^7 + C^{10}); 19.2 (C^1).

UV-Vis (MeOH, $2.4\cdot10^{-3}$ M): λ_{max}/nm (ε/$M^{-1}\cdot cm^{-1}$) = 240 (10^4), 292 (10^4), 328sh ($5.8\cdot10^3$), 390br ($1.6\cdot10^3$). Λ_m (MeOH, $2.4\cdot10^{-3}$ M): 11 $S\cdot cm^2\cdot mol^{-1}$.

[RuI(κ²*N*-{ONC(CH₂)₄CNOH})(η⁶-*p*-cymene)], 3^{-H}(Chart 9).

Chart 9. Structure of **3^{-H}**(numbering refers to carbon atoms).

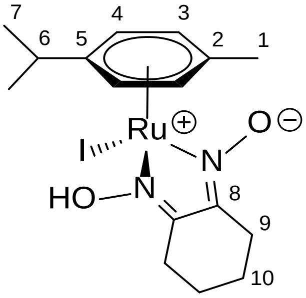

Preparedfrom [RuI$_2$(η^6-*p*-cymene)]$_2$ (53 mg, 0.054 mmol), nioxime (16 mg, 0.11 mmol) and NaHCO$_3$ (10 mg, 0.12 mmol), according to procedure D. Orange solid, yield: 45 mg, 80 %. The insolubility of **3^{-H}** in CH$_2$Cl$_2$ and acetone prevented its purification from traces of sodium salts (as reveled by conductivity and CHN analyses). Therefore, an alternative strategy was adopted. A suspension of [RuI$_2$(η^6-*p*-cymene)]$_2$ (160 mg, 0.164 mmol) and nioxime (47 mg, 0.33 mmol) in MeOH (10 mL) was stirred at room temperature for 1.5 h. The resulting red-brown solution was treated with Ag$_2$O (38 mg, 0.17 mmol) and stirred at room temperature for 2.5 h under protection from the light. The amber orange suspension was diluted with MeOH and filtered over celite. The orange filtrate was taken to dryness under vacuum and the residue was triturated in acetone/Et$_2$O 1:1 v/v. The suspension was filtered and the resulting orange solid was washed with Et$_2$O, hexane and dried under vacuum (40 °C). Yield: 129 mg, 78 %. Fairly soluble in MeOH, less soluble in EtOH, DMSO, insoluble in CH$_2$Cl$_2$, acetone, diethyl ether, hexane. Anal. Calcd. for $C_{16}H_{23}IN_2O_2Ru$: C, 38.18; H, 4.61; N, 5.57. Found: C, 37.12; H, 4.56; N, 5.38. IR (solid state): $\tilde{\upsilon}$/cm^{-1} = 3080w, 3039w, 2961m, 2940m, 2862m, 2800-2400m-br, 1498w, 1461m-sh, 1438s, 1423s-sh, 1388m, 1380m, 1369s, 1359s, 1298s, 1280m-sh, 1247w, 1232w, 1176s, 1159s-sh, 1109s (N=O), 1088s-sh, 1075m-sh, 1063m, 1035s (N-O), 1019s, 1003s-sh, 988s-sh, 969s, 943m-sh, 927m-sh, 902s, 896s, 883m-sh, 858s, 795s, 756m, 744ss, 690w, 665m. ^{1}H NMR (CD$_3$OD): δ/ppm = 5.67 (d,

$^3J_{HH}$ = 6.3 Hz, 2H, C^4H), 5.38 (d, $^3J_{HH}$ = 6.2 Hz, 2H, C^3H), 2.87 (hept, $^3J_{HH}$ = 6.9 Hz, 1H, C^6H), 2.71–2.56 (m, 4H, C^9H), 2.48 (s, 3H, C^1H), 1.63–1.51 (m, 4H, $C^{10}H$), 1.17 (d, $^3J_{HH}$ = 6.9 Hz, 6H, C^7H). $^{13}C\{^1H\}$ NMR (CD_3OD): δ/ppm = 105.6 (C^5), 104.4 (C^2), 88.9 (C^4), 86.5 (C^3), 32.9 (C^6), 26.6 (C^9), 22.5 (C^7 + C^{10}), 21.4 (C^1). The resonance of C^8 was not detected due to limited solubility. UV-Vis (MeOH, $2.0\cdot10^{-3}$ M): λ_{max}/nm (ε/$M^{-1}\cdot cm^{-1}$) = 290 ($7.3\cdot10^3$), 418 ($8.4\cdot10^2$). Λ_m (MeOH, $2.0\cdot10^{-3}$ M): 10 $S\cdot cm^2\cdot mol^{-1}$.

[RuCl(κ^2*N*-{ONC(CH_3)C(CH_3)NOH})(η^6-C_6Me_6)], 4^{-H}(Chart 10).

Chart 10. Structure of $\mathbf{4^{-H}}$ (numbering refers to carbon atoms).

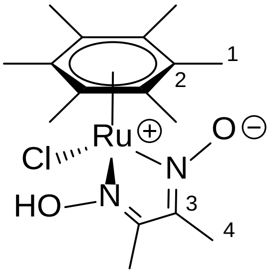

Prepared from [$RuCl_2(\eta^6-C_6Me_6)]_2$ (55 mg, 0.082 mmol), dimethylglyoxime (20 mg, 0.17 mmol) and $NaHCO_3$ (14 mg, 0.17 mmol),according to procedure D. Yellow solid, yield: 60 mg, 88 %. Soluble in CH_2Cl_2, MeOH, poorly soluble in Et_2O, insoluble in hexane. X-ray quality crystals of $\mathbf{4^{-H}}\cdot1.5H_2O$were obtained from a solution of [**4**]NO_3in EtOH, layered with Et_2O and stored at –20 °C. Anal. Calcd. for $C_{16}H_{25}ClN_2O_2Ru$: C, 46.43; H, 6.09; N, 6.77. Found: C, 44.05; H, 6.01; N, 6.65.IR (solid state): ṽ/cm^{-1} = 3019w, 2998w, 2979w, 2914w, 1613w-sh, 1556w, 1440s, 1380s, 1363m-sh, 1213m-sh, 1186s, 1109s (N=O), 1069m, 1041s (N-O), 1010s-sh, 993s-sh, 955s, 920m-sh, 832w-sh, 735m, 720m, 703m. ^1H NMR (CD_3OD): δ/ppm = 2.12 (s, 18H, C^1H); 2.10 (s, 6H, C^4H). No changes were observed in the ^1H NMR spectrum after a few days at room temperature. $^{13}C\{^1H\}$ NMR (CD_3OD): δ/ppm = 164.7 (C^3), 98.7 (C^2), 15.5 (C^1), 12.8 (C^4). UV-Vis (MeOH, $1.9\cdot10^{-3}$ M): λ_{max}/nm (ε/$M^{-1}\cdot cm^{-1}$) = 238 ($1\cdot10^4$), 294 ($6.2\cdot10^3$), 328sh ($4.1\cdot10^3$), 387br ($1.4\cdot10^3$). Λ_m (MeOH, $1.9\cdot10^{-3}$ M): 11 $S\cdot cm^2\cdot mol^{-1}$.

4.3. X-ray crystallography.

Crystal data and collection details for [**3**]NO_3,[**4**]$NO_3\cdot H_2O$and $\mathbf{4}^{\mathbf{-H}}\cdot 1.5H_2O$ are reported in Table 5. Data were recorded on a Bruker APEX II diffractometer equipped with a PHOTON2 detector using Mo–Kα radiation. The structures were solved by direct methods and refined by full-matrix least-squares based on all data using F^2.[57] Hydrogen atoms were fixed at calculated positions and refined using a riding model, except O-bonded hydrogens that have been located in the difference Fourier map and refined isotropically.

Table 5. Crystal data and measurement details for [**3**]NO_3,[**4**]$NO_3\cdot H_2O$ and $\mathbf{4}^{\mathbf{-H}}\cdot 1.5H_2O$.

Compound	[**3**]NO_3	[**4**]$NO_3\cdot H_2O$	$\mathbf{4}^{\mathbf{-H}}\cdot 1.5H_2O$
Formula	$C_{16}H_{24}IN_3O_5Ru$	$C_{16}H_{28}ClN_3O_6Ru$	$C_{16}H_{28}ClN_2O_{3.5}Ru$
FW	566.35	494.93	440.92
T, K	100(2)	100(2)	100(2)
λ,Å	0.71073	0.71073	0.71073
Crystal system	Orthorhombic	Orthorhombic	Monoclinic
Space group	*Pbca*	$Pca2_1$	$P2_1/c$
a, Å	14.031(6)	10.1596(7)	15.4589(10)
b, Å	14.473(6)	11.7047(8)	13.1592(8)
c, Å	19.564(7)	16.3630(11)	17.7332(11)
α,°	90	90	90
β,°	90	90	98.356(2)
γ,°	90	90	90
Cell Volume, Å^3	3973(3)	1945.8(2)	3569.1(4)
Z	8	4	8
D_c, g·cm^{-3}	1.894	1.689	1.641
μ, mm^{-1}	2.374	0.981	1.047
F(000)	2224	1016	1816
Crystal size, mm	0.18×0.14×0.10	0.18×0.12×0.10	0.22×0.19×0.15
θ limits,°	2.082-26.999	2.655-26.995	1.934-25.398
Reflections collected	55908	22857	59880
Independent reflections	4294 [R_{int} = 0.0402]	4221 [R_{int} = 0.0326]	6515 [R_{int} = 0.0508]
Data / restraints /parameters	4294 / 0 / 240	4221 / 3 / 260	6515 / 8 / 464
Goodness on fit on F^2 [a]	1.323	1.142	1.078
R_1 ($I > 2\sigma(I)$)[b]	0.0339	0.0239	0.0195
wR_2 (all data) [c]	0.0595	0.0528	0.0468
Largest diff. peak and hole, e Å^{-3}	0.876 / –0.858	0.435 / –0.400	0.401 / –0.323

[a] Goodness on fit on $F^2 = [\Sigma w(F_O^2 - F_C^2)^2/(N_{ref} - N_{param})]^{1/2}$, where $w = 1/[\sigma^2(F_O^2) + (aP)^2 + bP]$, where $P = (F_O^2 + 2F_C^2)/3$; N_{ref} = number of reflections used in the refinement; N_{param} = number of refined parameters. [b] $R_1 = \Sigma||F_O| - |F_C||/\Sigma|F_O|$. [c] $wR_2 = [\Sigma w(F_O^2 - F_C^2)^2/\Sigma w(F_O^2)^2]^{1/2}$, where $w = 1/[\sigma^2(F_O^2) + (aP)^2 + bP]$, where $P = (F_O^2 + 2F_C^2)/3$.

4.4. Reactivitystudies in MeOH.

General procedures are described below; experimental details and NMR data are reported in the ESI, NMR and MS spectra are given in Figures S42-S49.

1) with Brønsted bases. A solution of thedioxime compound (*ca*. 20 mg) in MeOH (2 mL) was treated with the selected base (up to 2.0 equivalents) and stirred at room temperature for 3-8 h. Addition of ^{t}BuOK was performed from a 1 M THF solution in anhydrous MeOH under N_2. Volatiles were removed under vacuum and the yellow/brown residue was analyzed by ^{1}H NMR (CD_3OD). The NMR tube was kept at room temperature overnight (14-18 h) and a new^{1}H NMR spectrum was recorded.

2) with silver nitrate. A solution of dioxime compound (*ca*. 15 mg) in MeOH (2 mL) was treated with $AgNO_3$ (1.0 equivalent) and stirred at room temperature for 1 h under protection from the light. A light grey/yellow solid (silver halide) was separated by filtration over celite. The filtrate solution was taken to dryness under vacuum and the brown residue was analyzed by ^{1}H NMR (CD_3OD). The NMR tube was kept at room temperature overnight (*ca*. 14 h) and the ^{1}H NMR spectrum was recorded.

Reactivity under catalytically relevant conditions. In a 10-mL test tube under N_2, a solution of [**3**]NO_3 or [**5**]NO_3 (*ca*. 15 mg) in anhydrous MeOH (2 mL) was treated with $PhNO_2$ and ^{t}BuOK (20 eq. each). The dark brown solution was stirred at room temperature for 1 h then at reflux for 20 h and finally analyzed by ^{1}H NMR and ^{1}H-^{13}C HMBC (CD_3OD). An analogous experiment was carried out using $PhNH_2$ instead of $PhNO_2$. In both cases, the selective formation of $[\mathbf{3}^{-2H}]^-$ or $[\mathbf{5}^{-2H}]^-$ was observed at room temperature. Progressive release of the η^6-arene ligand was observed over time (*p*-cymene: *ca*. 50 % after 6 h and almost quantitative after 20 h; C_6Me_6: 80 % after 20 h).

4.5. Catalytic activity.

The catalytic *N*-methylation reactions were carried out under a N_2 atmosphere in a pressure tube equipped with aTeflonhigh vacuum stopcock. Inside a glove box, an ovendried reactor was charged with the nitrocompound (0.5 mmol), the base (^{t}BuOK 0.5 mmol), and the catalyst (0.02 mmol, 4 mol%), dissolved in dry methanol (1 mL). After sealing, the reactor was purged threetimes with nitrogen and then pressurized with 1 atm of nitrogen.The resulting mixture was stirred at room temperature until complete dissolution of the catalyst and then placed in a thermostated oil bath at 130 °C. After 18h, it was left to cool to RT and the conversion and selectivity were determined by gas chromatography (GC-FID). The *N*-methylanilines were isolated by the following procedure. After the completion of the reaction, the reaction mixture was cooled to room temperature and filtrated through a pad of celite. After evaporating the solvent through rotary evaporator, the residue was eluted through a silica gel column using hexane/diethyl ether (typically 9:1*v*/*v*) as eluent. The fraction containing the product was salified with 4 M HCl in dioxane. After the removal of volatiles under vacuum,the pure *N*-methylaniline hydrochloride salt was dissolved in 0.5 mL of D_2O or $CDCl_3$ and analyzed by ^{1}H and ^{13}CNMR (Figures S50-S66).

Conflicts of interest. The authors declare no competing financial interest.

Acknowledgements.

L.B., F.M. and G.P. thank the University of Pisa for financial support under the "PRA 2022-2023 – *Progetti di Ricerca di Ateneo*" (Institutional Research Grants) - Project no. PRA_2022_12 "*New challenges of transition metal and lanthanide complexes in the perspective of green chemistry*". A.D.G thank the University of L'Aquila for financial support under the program "Progetti di ricerca di Ateneo 2021-2022".

Supporting Information (ESI).

Optimized preparation of $[RuCl_2(\eta^6\text{-arene})]_2$ (arene = *p*-cymene, C_6Me_6, 1,3,5-$C_6H_3Me_3$) and other ruthenium reference compounds. Solid-state IR and multinuclear NMR spectra of dioxime and oxime-oximato complexes. Comparison of IR and NMR data. X-ray data for hydrogen bonding in[**3**]NO_3, [**4**]NO_3, $\mathbf{4}^{\mathbf{-H}}\cdot 1.5H_2O$. Reactivitystudies in MeOH (NMR and MS data and spectra). Isolation and NMR characterization of *N*-methylated amines. Catalytic protocols and control experiments.

CCDC reference numbers 2241206([**3**]NO_3), 2241207([**4**]NO_3) and 2241208($\mathbf{4}^{\mathbf{-H}}\cdot 1.5H_2O$) contain the supplementary crystallographic data for the X-ray studies reported in this paper. These data can be obtained free of charge at https://www.ccdc.cam.ac.uk/structures/ or from the Cambridge Crystallographic Data Centre, 12, Union Road, Cambridge CB2 1EZ, UK; e-mail: deposit@ccdc.cam.ac.uk.

Notes and References.

---

[1] S. A. Lawrence, Amines:Synthesis Properties and Applications,*Cambridge University Press*, Cambridge, U.K., 2004.

[2] (a) Y. Chen, Recent Advances in Methylation: A Guide for Selecting Methylation Reagents, *Chem. Eur. J.* 2019, **25**, 3405–3439. (b) J. Chatterjee, F. RechenmacherandH. Kessler, N-Methylation of Peptides and Proteins: An Important Element for Modulating Biological Functions, *Angew. Chem. Int. Ed*. 2013, **52**, 254-269; (c) A. F.B. Räder, F. Reichart, M. Weinmüllerand H. Kessler, Improving oral bioavailability of cyclic peptides by N-methylation, *Bioorg. Med. Chem*. 2018, **26**, 2766-2773.

[3] (a) X. Wang, K. Zhao, H. Wangand F. Shi, Selective synthesis of N-monomethyl amines with primary amines and nitro compounds, *Catal. Sci. Technol*. 2021, **11**, 7239-7254 (b) V. Goyal, N. Sarki, A. Narani, G. Naik, K. NatteandR. V. Jagadeesh, Recent advances in the catalytic N-methylation and N-trideuteromethylation reactions using methanol and deuterated methanol, *Coord. Chem. Rev*. 2023,**474**, 214827.

[4] With reference to the ΔH° (25 °C) of the hydrogenation reaction of the corresponding aldehyde/ketone.(a) K. B. Wiberg, L. S. Crockerand K. M. Morgan, Thermochemical studies of carbonyl compounds. 5. Enthalpies of reduction of carbonyl groups, *J. Am. Chem. Soc*. 1991, **113**, 9,

---

3447–3450. (b) J. B. Pedley, R. D. NaylorandS. P. Kirby, *Thermochemical data of Organic Compounds*, 2nd ed.; Chapman and Hall: London, 1986.

[5] (a) G. Chelucci, Ruthenium and osmium complexes in CAC bond-forming reactionsby borrowing hydrogen catalysis, *Coord. Chem. Rev*., 2017,**331**, 1–36;(b) E. Podyacheva, O. I. Afanasyev, D. V. Vasilyevand D. Chusov, Borrowing Hydrogen Amination Reactions: A Complex Analysis of Trends and Correlations of the Various Reaction Parameters, *ACS Catal*. 2022, **12**, 7142−7198.

[6] K. Huh, Y. Tsuji, M. Kobayashi, F. Okudaand Y. Watanabe, Ruthenium catalyzed N-methylation of aminoarenes using methanol, *Chem. Lett*. 1988, **17**, 449-452

[7] (a)A. Del Zotto, W. Baratta, M. Sandri, G. Verardoand P. Rigo, Cyclopentadienyl RuII Complexes as Highly Efficient Catalysts for the N-Methylation of Alkylamines by Methanol, *Eur. J. Inorg. Chem*. 2004, 524-529;(b) S. Naskarand M. Bhattacharjee, Selective N-monoalkylation of anilines catalyzed by acationic ruthenium(II) compound, *Tetr. Lett*.,2007, **48**, 3367–3370;(c) T. T. Dang, B. Ramalingamand A. M. Seayad, Efficient Ruthenium-Catalyzed N-Methylation of Amines Using Methanol, *ACS Catal*. 2015, **5**, 4082−4088;(d)G. Choiand S. H. Hong, Selective Monomethylation of Amines with Methanol as the C1 Source, *Angew. Chem. Int. Ed*. 2018, **57**, 6166 –6170;(e)M. Maji, K. Chakrabarti, B. Paul, B. Chandra Royand S. Kundu, Ruthenium(II)-NNN-Pincer-Complex-Catalyzed Reactions Between Various Alcohols and Amines for Sustainable CN and CC Bond Formation, *Adv. Synth. Catal*. 2018, **360**, 722 –729;(f)B. Chandra Roy, S. Debnath, K. Chakrabarti, B. Paul, M. Majiand S. Kundu, ortho-Amino group functionalized 2,2'-bipyridine based Ru(II) complex catalysed alkylation of secondary alcohols, nitriles and amines using alcohols, *Org. Chem. Front*., 2018, **5**, 1008; (g)O. Ogata, H. Nara, M. Fujiwhara, K. Matsumuraand Y. Kayaki, N-Monomethylation of Aromatic Amines with Methanol via PNHP-Pincer Ru Catalysts, *Org. Lett.* 2018, **20**, 3866−3870;(h) K. Das, P. Gobinda Nandi, K. Islam, H. Kumar Srivastavaand A. Kumar, N–Alkylation of Amines Catalyzed by a Ruthenium–Pincer Complex in the Presence of in situ Generated Sodium Alkoxide, *Eur. J. Org. Chem*. 2019, 6855–6866;(i) N. Biswasand D. Srimani, Ru-Catalyzed Selective Catalytic Methylation and MethylenationReaction Employing Methanol as the C1 Source, *J. Org. Chem*. 2021, **86**, 10544−10554.

---

[8] (a) L. M. Broomfield, Y. Wu, E. Martinand A. Shafir, Phosphino-amine (PN) Ligands for Rapid Catalyst Discovery in Ruthenium-Catalyzed Hydrogen-Borrowing Alkylation of Anilines: A Proof of Principle*Adv. Synth. Catal*. 2015, **357**, 3538–3548; (b) S. N. R.Donthireddy,P. Mathoor IllamandA. Rit, Ruthenium(II) Complexes of Heteroditopic N-Heterocyclic Carbene Ligands: Efficient Catalysts for C−N Bond Formation via a HydrogenBorrowing Strategy under Solvent-Free Conditions,*Inorg. Chem*. 2020, **59**, 1835−1847;(c)P. Piehl, R. Amuso, A. Spannenberg, B. Gabriele, H. Neumannand M. Beller, Efficient methylation of anilines with methanol catalysed by cyclometalated ruthenium complexes, *Catal. Sci. Technol.*, 2021, **11**, 2512;(d)P. Liu,N. Thanh Tung, X. Xu, J. Yangand F. Li, N-Methylation of Amines with Methanol in the Presence of Carbonate Salt Catalyzed by a Metal−Ligand Bifunctional Ruthenium Catalyst [(p-cymene)Ru(2,2′-bpyO)(H2O)], *J. Org. Chem.* 2021, **86**, 2621−2631;(e)M. Huang,Y. Li, X.-B. Lan,J. Liu,C. Zhao,Y. Liuand Z. Ke, Ruthenium(II) complexes with N-heterocyclic carbene–phosphine ligands for the N-alkylation of amines with alcohols,*Org. Biomol. Chem*., 2021, **19**, 3451;(f) P. Mathoor Illamand Arnab Rit, Electronically tuneableorthometalatedRuII–NHCcomplexes as efficient catalysts for C–C and C–N bond formations via borrowing hydrogenstrategy, *Catal. Sci. Technol*., 2022, **12**, 67;(g) S. Dindar,A. Nemati Kharatand A. Abbasi, Green and chemo selective amine methylation using methanol by anorganometallic ruthenium complex, *J. Organomet. Chem.*, 2022, **957**, 122155.

[9] C. Meng, P. Liu, N. Thanh Tung, X. Hanand F. Li, N-Methylation of Amines with Methanol in Aqueous Solution Catalyzed by a Water-Soluble Metal−Ligand Bifunctional Dinuclear Iridium Catalyst, *J. Org. Chem.* 2020, **85**, 5815−5824

[10] (a) R. V. Jagadeesh, A. E. Surkus, H. Junge, M. M. Pohl, J. Radnik, J. Rabeah, H. M. Huan, V. Schunemann, A. BrucknerandM. Beller, Nanoscale Fe2O3-Based Catalysts for Selective Hydrogenation of Nitroarenes to Anilines, *Science* 2013, **342**, 1073-1076; (b) G. Booth, Nitro Compounds, Aromatic. In *Ullmann's Encyclopedia of Industrial Chemistry*, 2000, Ed. Wiley-VCH

[11] (a) D. Wangand D. Astruc, The Golden Age of Transfer Hydrogenation, *Chem. Rev*. 2015, **115**, 6621−6686; (b) R. Noyoriand S. Hashiguchi,Asymmetric Transfer Hydrogenation Catalyzed by Chiral Ruthenium Complexes,*Acc. Chem. Res*. 1997, **30**, 97–102

---

[12] (a) B. Paul, S. Shee, K. Chakrabartiand S. Kundu, Tandem Transformation of Nitro Compounds intoN-Methylated Amines: Greener Strategy for the Utilization of Methanol as a Methylating Agent, *ChemSusChem* 2017, **10**, 2370–2374; (b) S. Zhang, J. Juweriah Ibrahimaand Y. Yang, A pincer ligand enabled ruthenium catalyzed highly selective N-monomethylation of nitroarenes with methanol as the C1 source, *Org. Chem. Front*., 2019, **6**, 2726–2731; (c) N. Sarki, V. Goyal, N. Kumar Tyagi, Puttaswamy, A. Narani, A. Rayand K. Natte, Simple RuCl3-catalyzed N-Methylation of Amines and Transfer Hydrogenation of Nitroarenes using Methanol, *ChemCatChem* 2021, **13**, 1722–1729; (d) K. Li, J.-F. Li, B. Yinand F. Zeng, Investigation of NNN Pincer Ruthenium(II) Complexes with a Pendant Hydroxyl Group for N-Monomethylation of amines and Nitroarenes by Methanol, *ChemCatChem* 2022, **14**, e202101630.

[13] L. Biancalana, I. Abdalghani, F. Chiellini, S. Zacchini, G. Pampaloni, M. Crucianelliand F. Marchetti, Ruthenium Arene Complexes with α-Aminoacidato Ligands: New Insights into Transfer Hydrogenation Reactions and Cytotoxic Behaviour, *Eur. J. Inorg. Chem*. 2018, 3041–3057

[14] Selected references: (a) U. Kolle, E. Raabeb, C. Kriigerbundand F. P. Rotzinger, MetallorganischeMonoglyoximato-Komplexevon Co und Rh, *Chem. Ber*. 1987, **120**, 979-985. (b) E. N. Treher, L. C. Francesconi, J. Z. Gougoutas, M. F. Malleyand A. D. Nunn,Monocapped tris(dioxime) complexes of technetium(III): synthesis and structural characterization of TcX(dioxime)3B-R (X = Cl, Br; dioxime = dimethylglyoxime, cyclohexanedione dioxime; R = CH3, C4H9), *Inorg. Chem*. 1989, **28**, 18, 3411–3416. (c) Y. Z.Voloshin, A. Varzatskii, A. V.Palchik, E. V.Polshin, Y. A. Maletinand N. G. Strizhakova, Synthesis, spectral and electrochemical characteristics of asymmetrical iron(II) tris-dioximates, *Polyhedron* 1998, **17**, 4315-4326. (d) V. Yu. Kukushkin, T. B. Pakhomova, N. A. Bokach, G. Wagner, M. L. Kuznetsov, M. Sophia Galanskiand A. J. L. Pombeiro, Iminoacylation. 3. Formation of Platinum(IV)-Based Metallaligands Due to Facile One-End Addition of Wic-Dioximes to Coordinated Organonitriles, *Inorg. Chem*. 2000, **39**, 216-225. (e) R. Llanguri, J. J. Morris, W. C. Stanley, E. T. Bell-Loncell, M. Turner, W. J. Boykoand C. A. Bessel, Electrochemical and spectroscopic investigations of oxime complexes of bis(bipyridyl)ruthenium(II), *Inorg. Chim. Acta, 2001*,**315**, 53–65.

---

[15] D. Dolui, S. Khandelwal, P. Majumderand A. Dutta, The odyssey of cobaloximes for catalytic H2 production and their recent revival with enzyme-inspired design, *Chem. Commun*., 2020, **56**, 8166.

[16] (a) L. Tschugaeff, Uebereinneues, empfindlichesReagens auf Nickel**,** Chem. Ber. 1905, **38**, 2520-2522. (b) R. C. Voter, C. V. Banksand H. Diehl, 1,2-Cyclohexanedione dioxime - A reagent for Nickel, *Anal. Chem*. 1948, **20**, 5, 458–460.

[17] To the best of our knowledge, the following are the catalytic studies published so far on ruthenium dioxime compounds. The papers are all related to *trans*-$[RuX_2(\kappa^2 N\text{-}\{ONC(R)C(R)NOH\})]^-$ complexes (R = Me, Ph; X = Cl, ClO_4) as catalytic precursors for water oxidation and olefin epoxidation. (a) M. M. Taqui Khan, G. Ramachandraiahand S. H. Mehta, trans-dioxo-bis(dimethylglyoximato)ruthenium(VII) perchlorate: an active oxidation catalyst for the electrochemical epoxidation of olefins. *J. Mol. Cat.* 1989, **50**, 123-129 (b) M. M. Taqui Khan, G. Ramachandraiah, S. H. Mehta, S. H. R. Ardiand S. Kumar, Mononuclear Bis(dimethylglyoximato)Ruthenium(III) complexes with different appended axial groups: highly efficient catalysts for water oxidation. *J. Mol. Cat*. 1990, **58**, 199-203. (c) M. M. Taqui Khan, D. Chatterjee, N. H. Khan, R. I. Kureshiand K. N. Bhatt Epoxidation of cyclohexene with iodosylbenzenecatalysed by Ru(III)-dmg and Ru(III)-dpg complexes: synthesis and characterisation of catalytically active Ru(V)-oxo intermediates. *J. Mol. Cat*. 1992, **77**, 153-158.

[18] (a) M. S. Ibn El Alami, M. A. El Amrani, A. Dahdouh, P. Roussel, I. Suisseand A. Mortreux, α-Amino-Oximes Based on Optically Pure Limonene: A New Ligands Family for Ruthenium-Catalyzed Asymmetric Transfer Hydrogenation, *Chirality* 2012, **24**, 675-682. (b) J. Francos, L. Menendez-Rodriguez, E. Tomas-Mendivil, P. Crochetand V. Cadierno, Synthesis and catalytic applications of ruthenium(II)–phosphino-oxime complexes, *RSC Adv*., 2016, **6**, 39044. (c) D. Tyagi, R. Kumar Rai, S. M. Mobinand S. Kumar Singh, N-Substituted Iminiopyridine Arene-ruthenium Complexes for the Regioselective Catalytic Hydration of Terminal Alkynes, *AsianJ. Org. Chem.* 2017, **6**, 1647-1658. (d) M. Kumar Awasthi, D. Tyagi, S. Patra, R. Kumar Rai, S. M. Mobinand S. Kumar Singh, Ruthenium Complexes for Catalytic Dehydrogenation of Hydrazine and Transfer Hydrogenation Reactions, *Chem. Asian J.* 2018, **13**, 1424–1431. (e) V. V. Matveevskaya, D. I. Pavlov, T. S. Sukhikh, A. L. Gushchin, A. Yu. Ivanov, T. B. Tennikova, V. V. Sharoyko, S. V.

Baykov, E. Benassi and A. S. Potapov, Arene−Ruthenium(II) Complexes Containing 11H-Indeno[1,2-b]quinoxalin-11-one Derivatives and Tryptanthrin-6-oxime: Synthesis, Characterization, Cytotoxicity, and Catalytic Transfer Hydrogenation of Aryl Ketones, *ACS Omega* 2020, **5**, 11167−11179.

[19] (a) M. Iglesias, C. Del Pino, A. Corma, S. Garcia-Blancoand S. Martinez Carrera, Rhodium Complexes with Phosphine and Diazabutadiene Ligands. Their Properties as Hydrogenation Catalysts. Molecular Structure of RhCI(COD)P(p-C6H4F)3, *Inorg. Chim. Acta* 1987, **127**, 215-221. (b) M. Bikrani, L. Fidalgoand M. A. Garralda, Iridium complexes with α-diimines: Catalytic hydrogen transfer from isopropanol to cyclohexanone, *Polyhedron* 1996, **15**, 83-89.(c) M. Bikrani, L. Fidalgo, M. A. Garraldaand C. Ubide, Catalytic hydrogen transfer activity of cationic iridium(I) complexes containing a-diimines, *J. Mol. Cat. A. Chem*. 1997, **18**, 47-53. (d) M. Moszner, A. M. Trzeciakand J. J. Ziołkowski, Rhodium complexes with dioximes as catalysts of hydroformylation and hydrogenation of 1-hexene, *J. Mol. Cat. A. Chem*. 1998, **130**, 241–248.(e) B. Berchtold, V. Lozan, P.-G. Lassahnand C. Janiak, Nickel(II) and Palladium(II) Complexes with -Dioxime Ligands as Catalysts for the Vinyl Polymerization of Norbornene in Combination with Methylaluminoxane, Tris(pentafluorophenyl)borane, or Triethylaluminum Cocatalyst Systems, *J. Polym. Sci. A. Polym. Chem*. 2002, **40**, 3604–3614.(f) T. Ganicz, U. Mizerska, M. Moszner, M. O’Brien, R. Perryand W. A. Stanczyk, The effectiveness of rhodium(I), (II) and (III) complexes as catalysts in hydrosilylation of model olefin and polyether with triethoxysilane and poly(dimethylsiloxane-co-methylsiloxane), *App. Cat. A:General*, 2004, **259**, 49–55. (g) S. Iyer, G. M. Kulkarniand C. Ramesh, Mizoroki–Heck reaction, catalysis by nitrogen ligand Pd complexes and activation of aryl bromides, *Tetrahedron* 2004, **60**, 2163–2172.

[20] S.-M. Lu, Z. Wang, J. Wang, J. Li and C. Li, Hydrogen generation from formic acid decomposition on a highly efficient iridium catalyst bearing a diaminoglyoxime ligand, *Green Chem*., 2018, **20**, 1835.

[21] Only [RuCl(MeCN)$_2$(η^6-*p*-cymene)]PF$_6$ has been previously isolated and characterized. (a) S. B. Jensen, S. J. Rodgerand M. D. Spicer, Facile preparation of η^6-p-cymene ruthenium diphosphine complexes. Crystal structure of [(η^6-p-cymene)Ru(dppf)Cl]PF6, *J. Organomet. Chem*.,1998, **556**,

---

151–158. (b) R. E. Morris, R. E. Aird, P. d. S. Murdoch, H. Chen, J. Cummings, N. D. Hughes, S. Parsons, A. Parkin, G. Boyd, D. I. JodrellandP. J. Sadler, Inhibition of Cancer Cell Growth by Ruthenium(II) Arene Complexes, *J. Med. Chem*. 2001, **44**, 3616-3621.

[22] The resonance for the OH groups was not detected due to rapid H/D exchange with the solvent.

[23] G. Orellana, C. Alvarez Ibarraand J. Santoro, 1H and 13C NMR Coordination-Induced Shifts in a Series of Tris(tt-diimine)ruthenium(II) Complexes Containing Pyridine, Pyrazine, and Thiazole Moieties, *Inorg. Chem.* 1988, **27**, 6, 1025–1030

[24] A. Palm and H. Werbin, The Infrared Spectra of Alpha and Beta Oximes,*Can. J. Chem.*, 1953, **31**, 1004-1008

[25] P. Kumar, A. K. Singh, S. Sharma and D. S. Pandey, *J. Organomet. Chem*. 2009, **694**, 3643-3652.

[26] (a) R. Bergs, R. Lampeka, C. Robland W. Beck, Halbsandwichkomplexe von Iridium(III) und Ruthenium(II) mitDianionen von 2-Hydroxyiminocarbonsäuren, *Z. Naturforsch*. 1994, **49b**, 483-488. (b) R. Lampeka, R. Bergs, R. Krämer, K. Polbornand W. Beck, Halbsandwichkomplexe von Cobalt(III), Rhodium(III), Iridium(III) und Ruthenium(II) mitAnionen von cx-Hydroxyiminosäuren, *Z. Naturforsch*., 1994, **49b**, 225-232.

[27] (a) L. F. Szczepura, J. G. Muller, C. A. Bessel, R. F. See, T. S. Janik, M. R. Churchilland K. J. Takeuchi, Characterization of protonated trans bis(dioxime) ruthenium complexes: crystal structures of trans-Ru(DPGH)2(NO)Cl, trans-[Ru(DMGH)(DMGH2)(NO)Cl]Cl, and trans-Ru(DMGH)2(NO)Cl, *Inorg. Chem*. 1992, **31**, 859-869. (b) A. K. Das, S.-M. Pengand S. Bhattacharya, Chemistry of ruthenium with some dioxime ligands. Syntheses, structures and reactivities, *Polyhedron* 2001, **20**, 327-335. (c) N. Chitrapriya, V. Mahalingam, M. Zeller, H. Leeand K. Natarajan, Synthesis, characterization, DNA binding and cleavage studies of Ru(II) complexes containing oxime ligands, *J. Mol. Struct*. 2010, **984**, 30-38.

[28] Y. Benabdelouahab, L. Muñoz-Moreno, M. Frik, I. de la Cueva-Alique, M. Amin El Amrani, M. Contel, A. M. Bajo, T. Cuencaand E. Royo, Hydrogen Bonding and Anticancer Properties of Water-Soluble Chiral p-Cymene RuII Compounds with Amino-Oxime Ligands, *Eur. J. Inorg. Chem*. 2015, 2295–2307.

---

[29] (a) L. Biancalana, L. K. Batchelor, G. Ciancaleoni, S. Zacchini, G. Pampaloni, P. J. Dysonand F. Marchetti, Versatile coordination of acetazolamide to ruthenium(II) p-cymene complexes and preliminary cytotoxicity studies, *Dalton Trans*., 2018, **47**, 9367-9384. (b) M. Kubanik, H. Holtkamp, T. Söhnel, S. M. F. Jamiesonand C. G. Hartinger, Impact of the Halogen Substitution Pattern on the Biological Activity of Organoruthenium 8-Hydroxyquinoline Anticancer Agents, *Organometallics* 2015, **34**, 5658−5668. (c) G. Zeng, S. Sakaki, K.-i. Fujita, H. Sanoand R. Yamaguchi, Efficient Catalyst for Acceptorless Alcohol Dehydrogenation: Interplay of Theoretical and Experimental Studies, *ACS Catal.* 2014, **4**, 1010−1020.

[30] (a) M. Watanabe, Y. Kashiwame, S. Kuwataand T. Ikariya, Synthesis, Structures, and Transfer Hydrogenation Catalysis of Bifunctional Iridium Complexes Bearing a C–N Chelate Oxime Ligand, *Eur. J. Inorg. Chem.* 2012, 504–511(b) T. Takamura, T. Harada, T. Furuta, T. Ikariyaand S. Kuwata, Half-Sandwich Iridium Complexes Bearing a Diprotic Glyoxime Ligand: Structural Diversity Induced by Reversible Deprotonation, *Chem. Asian J.* 2020, **15**, 72–78.

[31] Y. C. Wuand P. A. Berezansky, Low Electrolytic Conductivity Standards, *J. Res. Natl. Inst. Stand. Technol*., 1995, **100**, 521-527

[32] We do not imply arene dissociation from dioxime complexes can only occur after prior dissociation/removal of the halido ligand. See the stability studies of [**3**]NO_3 under catalytically-relevant conditions.

[33] L. Biancalana, E. Zanda, M. Hadiji, S. Zacchini, A. Pratesi, G. Pampaloni, P. J. Dysonand F. Marchetti, Role of the (pseudo)halido ligand in ruthenium(ii) p-cymene α-amino acid complexes in speciation, protein reactivity and cytotoxicity, *Dalton Trans*. 2021, **50**, 15760-15777 and references therein.

[34] As a matter of fact, the procedure for the selective formation of $\mathbf{2}^{-\mathbf{H}}$ required the use of a mild Brønsted base ($NaHCO_3$) in stoichiometric conditions with short reaction times (*vide supra*).

[35] C. Paaland W. Hartmann, Über den Einfluß von Fremdstoffen auf die Aktivität der Katalysatoren. IV. VersuchemitPalladiumhydrosol in Qegenwart von Queksilber und Quecksilberoxyd. Ber. Deutsch. *Ber. Dtsch. Chem. Ges*. 1918, **51**, 711–737.

---

[36] M. A. Bennettand A. K. Smith, Arene ruthenium(II) complexes formed by dehydrogenation of cyclohexadienes with ruthenium(III) trichloride, *J. Chem. Soc., Dalton Trans.*, 1974, 233-241.

[37] Some recent applications of the Noyori-Ikariya catalysts: (a) Q. Xing, C.-M. Chan, Y.-W. Yeungand W.-Y. Yu, Ruthenium(II)-Catalyzed Enantioselective γ-Lactams Formation by Intramolecular C–H Amidation of 1,4,2-Dioxazol-5-ones, *J. Am. Chem. Soc*. 2019, **141**, 9, 3849–3853. (b) T. Tougeand T. Arai, Asymmetric Hydrogenation of Unprotected Indoles Catalyzed by η6-Arene/N-Me-sulfonyldiamine–Ru(II) Complexes, *J. Am. Chem. Soc*. 2016, **138**, 35, 11299–11305. (c) Y. Li, S. Zhu, J. Liand A. Li, Asymmetric Total Syntheses of Aspidodasycarpine, Lonicerine, and the Proposed Structure of Lanciferine, *J. Am. Chem. Soc*. 2016, **138**, 12, 3982–3985. (d) L. Wu, R. Jin, L. Li, X. Hu, T. Chengand G. Liu, A Michael Addition–Asymmetric Transfer Hydrogenation One-Pot Enantioselective Tandem Process for Syntheses of Chiral γ-Secondary Amino Alcohols, *Org. Lett*. 2017, **19**, 12, 3047–3050. (e) A. M. R. Hall, P. Dong, A. Codina, J. P. Loweand U. Hintermair, Kinetics of Asymmetric Transfer Hydrogenation, Catalyst Deactivation, and Inhibition with Noyori Complexes As Revealed by Real-Time High-Resolution FlowNMR Spectroscopy, *ACS Catal.* 2019, **9**, 3, 2079–2090. (f) L.-R. Wang, D. Chang, Y. Feng, Y.-M. He, G.-J. Dengand Q.-H. Fan, Highly Enantioselective Ruthenium-Catalyzed Cascade Double Reduction Strategy: Construction of Structurally Diverse Julolidines and Their Analogues, *Org. Lett*. 2020, **22**, 6, 2251–2255. (g) G. S. Caleffi, J. de O. C. Brum, A. T. Costa, J. L. O. Domingosand P. R. R. Costa, Asymmetric Transfer Hydrogenation of Arylidene-Substituted Chromanones and Tetralones Catalyzed by Noyori–Ikariya Ru(II) Complexes: One-Pot Reduction of C═C and C═O bonds, *J. Org. Chem*. 2021, **86**, 6, 4849–4858.

[38] M. González-Lainez , M. V. Jiménez , V. Passarelli and J. J. Pérez-Torrente, Effective N-methylation of nitroarenes with methanol catalyzed by a functionalized NHC-based iridium catalyst: a green approach to N-methyl amines, *Catal. Sci. Technol*., 2020,**10**, 3458-3467

[39] B. Paul , K. Chakrabarti, S. Shee, M. Maji, A. Mishra and S. Kundu, A simple and efficient in situ generated ruthenium catalyst for chemoselective transfer hydrogenation of nitroarenes: kinetic and mechanistic studies and comparison with iridium systems, *RSC Adv*., 2016, **6**, 100532-100545.

---

[40] L. Wang , H. Neumann and M. Beller,Palladium-Catalyzed Methylation of Nitroarenes with Methanol, *Angew. Chem., Int. Ed*., 2019, **58**, 5417-5421.

[41] B. Chaudret, X. Heand Y. Huang, Selective Preparation of Unusual n-adducts of the Functional Arenes Diphenylacetylene, Phenol, and Benzoic Acid with the CpRu+ Fragment (Cp = C5Me5), *J. Chem. Soc. Chem. Commun*. 1989, 1844-1846

[42] Selected references: (a) M. Lari, M. Martínez-Alonso, N. Busto, B. R. Manzano, A. M. Rodríguez, M. I. Acuña, F. Domínguez, J. L. Albasanz, J. M. Leal, G. EspinoandB. García, Strong Influence of Ancillary Ligands Containing Benzothiazole or Benzimidazole Rings on Cytotoxicity and Photoactivation of Ru(II) Arene Complexes, *Inorg. Chem*. 2018, **57**, 14322−14336. (b) D. A. Freedman, S. Kruger, C. RoosaandC. Wymer, Synthesis, Characterization, and Reactivity of [Ru(bpy)(CH3CN)3(NO2)]PF6, a Synthon for [Ru(bpy)(L3)NO2] Complexes,*Inorg. Chem*. 2006, **45**, 9558−9568

[43] K.-J. Haack, S. Hashiguchi, A. Fujii, T. Ikariyaand R. Noyori, The Catalyst Precursor, Catalyst, and Intermediate in the RuII-Promoted Asymmetric Hydrogen Transfer between Alcohols and Ketones, *Angew. Chem Int. Ed*. 1997, **36**, 285-288

[44] Selected references: (a)M. Bassetti, F. Centola, D. Semeril, C.Bruneauand P. H. Dixneuf, Rate Studies and Mechanism of Ring-Closing Olefin Metathesis Catalyzed by Cationic Ruthenium Allenylidene Arene Complexes, *Organometallics* 2003, **22**, 4459-4466. (b) D.-H. Lee, K.-H. Kwonand C. S. Yi, Dehydrative C−H Alkylation and Alkenylation of Phenols with Alcohols: Expedient Synthesis for Substituted Phenols and Benzofurans, *J. Am. Chem. Soc*. 2012, **134**, 7325−7328. (c)T. Roggeand L. Ackermann, Arene-Free Ruthenium(II/IV)-Catalyzed Bifurcated Arylation for Oxidative C@H/C@H Functionalizations,*Angew. Chem. Int. Ed.*, 2019, **58**,15640-15645. (d) R. Chanerika , H. B. Friedrichand M. L. Shozi, Application of new Ru (II) pyridine-based complexes in the partial oxidation of n-octane, *Appl.Organomet. Chem*. 2020;**34**:e5361. (e) K. Salzmann, C. Segarraand M. Albrecht, Donor-Flexible Bis(pyridylidene amide) Ligands for Highly Efficient Ruthenium-Catalyzed Olefin Oxidation, *Angew. Chem. Int. Ed*. 2020, **59**, 8932–8936

[45] Following the procedure described in ref. 33, KI was used instead of NaI, 2 h reflux, 95 % isolated yield.

---

[46] E. Zanda, N. Busto, L. Biancalana, S. Zacchini, T. Biver, B. Garciaand F. Marchetti, Anticancer and antibacterial potential of robust Ruthenium(II) arene complexes regulated by choice of α-diimine and halide ligands, *Chem. Biol. Interact*. 2021, **344**, 109522.

[47] L. Biancalana, G. Pampaloni, S. Zacchiniand F. Marchetti, Synthesis, characterization and behavior in water/DMSO solution of Ru(II) arene complexes with bioactive carboxylates, *J. Organomet. Chem*. 2018, **869**, 201-211.

[48] (a) M. A. Bennett, T.-N. Huang, T. W. Mathesonand A. K. Smith, *Inorg. Synth*., 1982, **21**, 72–78. (b) S, L. Nongbri, B, Dasand K. Mohan Rao, *J. Organomet. Chem*., 2009, **694**, 3881–3891. (c) L. E. Heim, S. Vallazza, D. van der Waalsand M. H. G. Prechtl, *Green Chem*., 2016, **18**, 1469–1474.

[49] M. A. Bennett and J. P. Ennett, Synthesis and Spectroscopic Characterization of Dinuclear Mono(μ-hydrido) Arene Complexes of Divalent Ruthenium, *Organometallics* 1984, **3**, 1365-1374.

[50] B. Chatterjee and C. Gunanathan, *Chem. Commun*. 2014,**50**, 888-890.

[51] (a) W. Huber, P. Bröhler, W. Wätjen, W. Frank, B. Spingler and P. C. Kunz, Cytotoxicity of ruthenium(II) piano-stool complexes with imidazole-based PN ligands, *J. Organomet. Chem*., 2012,**717**, 187-194. (b) M.-L. Hu, V. Safarifard, A. Morsali, T.-L. Shao and X.-C. Li, Facile fabrication of ruthenium(IV) oxide nanostructures by thermal decomposition of two new organoruthenium(II) complexes, *Inorg. Chem. Commun*., 2013, **37**, 189–192.

[52] L. Evanno, J. Ormala and P. M. Pihko, A Highly Enantioselective Access to Tetrahydroisoquinoline and b-Carboline Alkaloids with Simple Noyori-Type Catalysts in Aqueous Media, *Chem. Eur. J.* 2009, **15**, 12963–12967.

[53] (a) R. K. Harris, E. D. Becker, S. M. Cabral De Menezes, R. Goodfellow and P. Granger, NMR nomenclature. Nuclear spin properties and conventions for chemical shifts (IUPAC Recommendations 2001), *Pure Appl. Chem*. 2001, **73**, 1795–1818. (b) G. R. Fulmer, A. J. M. Miller, N. H. Sherden, H. E. Gottlieb, A. Nudelman, B. M. Stoltz, J. E. Bercaw and K. I. Goldberg, NMR Chemical Shifts of Trace Impurities: Common Laboratory Solvents, Organics, and Gases in Deuterated Solvents Relevant to the Organometallic Chemist, *Organometallics*, 2010, **29**, 2176–2179.

---

[54] F. Menges, "Spectragryph - optical spectroscopy software", Version 1.2.16d, @ 2016-2020, http://www.effemm2.de/spectragryph.

[55] W. J. Geary, The Use of Conductivity Measurements in Organic Solvents for the Characterisation of Coordination Compounds, *Coord. Chem. Rev.*, 1971, **7**, 81-122.

[56] Limiting molar conductivity in MeOH: 114 S·cm^2·mol^{-1} for KNO_3 and 95 S·cm^2·mol^{-1} for $[Bu_4N]Br$ S·cm^2·mol^{-1}. Taken from: R. K. Boggess, D. A. Zatko, The use of conductivity data for the structure determination of metal complexes, *J. Chem. Educ*. 1975, **52**, 10, 649-651.

57 G. M. Sheldrick, Crystal structure refinement with SHELXL. *Acta Crystallogr. C*, 2015, **71**, 3-8.